


Lipopolyplex Ternary Delivery Systems Incorporating C14 Glycerol-Based Lipids

Laila Kudsiova,^{*,†} Barbara Fridrich,[†] Jimmy Ho,[‡] M. Firouz Mohd Mustapa,[‡] Frederick Campbell,[‡] Katharina Welser,[‡] Melanie Keppler,[§] Tony Ng,^{§,‡} David J. Barlow,[†] Alethea B. Tabor,[‡] Helen C. Hailes,[‡] and M. Jayne Lawrence[†]

[†]Institute of Pharmaceutical Science, King's College London, Franklin-Wilkins Building, 150 Stamford Street, Waterloo Campus, London SE1 9NH, U.K.

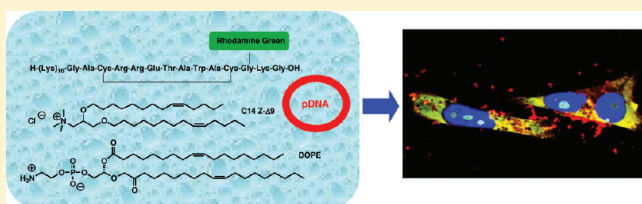
[‡]Department of Chemistry, University College London, 20 Gordon Street, London WC1H 0AJ, U.K.

[§]Randall Division of Cell and Molecular Biophysics, King's College London, Henriette Raphael Building, Guy's Campus, London SE1 1UL, U.K.

 Supporting Information

ABSTRACT: The structure, biophysical properties and biological behavior of lipopolyplex ternary gene delivery vectors incorporating novel C14 glycerol based lipids of varying alkyl chain geometry (containing cis, trans or alkyne double bonds) have been studied in the presence and absence of a bifunctional targeting peptide designed to both condense DNA and confer integrin-specific targeting. In vitro transfection studies in breast cancer MDA-MB-231 cells revealed that ternary formulations of lipid:peptide:DNA (LPD) complexes prepared using the aforementioned lipids possessed highly synergistic transfection activity up to 2500-fold higher than their respective lipid:DNA (LD) or peptide:DNA (PD) counterparts. Furthermore, the small structural differences in the lipid alkyl chain geometries also resulted in pronounced differences in transfection within each type of formulation, whereby the trans lipids showed best activity when formulated as LD complexes, whereas the cis lipids were superior in LPD formulations. Confocal fluorescence internalization studies using labeled components of the formulations showed both the lipid and the DNA of LD complexes to be trapped in endocytic compartments, whereas in the case of LPD complexes, the DNA was clearly released from the endosomal compartments and, together with the peptide, internalized within the cell nucleus. Physicochemical characterization of the formulations carried out by light and neutron scattering, zeta potential measurement, and negative staining electron microscopy detected major structural differences between LD and LPD complexes. Gel electrophoresis assays additionally showed differences between the individual lipids tested in each type of formulation. In conclusion, the superior transfection of the trans lipids in the LD complexes was thought to be attributed to superior DNA binding caused by a more closely matched charge distribution of the more rigid, trans lipids with the DNA. In the case of the LPD complexes, the DNA was thought to be predominantly condensed by the cationic portion of the peptide forming a central core surrounded by a lipid bilayer from which the targeting sequence partially protrudes. The more fluid, cis lipids were thought to confer better activity in this formulation due to allowing more of the targeting peptide sequence to protrude.

KEYWORDS: cationic lipid, targeting peptide, DNA delivery, lipoplex, lipopolyplex, gene therapy



1. INTRODUCTION

Gene therapy is currently one of the most promising strategies for developing cures to genetic and acquired diseases by correcting a genetic defect or expressing a therapeutic protein.¹ To date, however, the development of a gene delivery vector capable of providing the benefit of the high transfection efficacy displayed by viral vectors, while avoiding the toxicity and immunogenicity associated with these vectors, has proven very challenging. Although nonviral vectors are regarded as safer alternatives, their transfection efficiency is still relatively low^{2,3} due to a combination of lack of specificity and inability to overcome the numerous barriers to gene delivery.⁴ Despite these limitations, vectors formulated from cationic lipids (known as lipoplexes) have emerged

as one of the major nonviral gene delivery systems. They are capable of transfecting various cell types with relatively low immunogenicity and toxicity,^{5–7} and further surface modification, in particular through the addition of PEG or targeting ligands, is usually required to improve biological stability, targeting efficiency, cellular internalization and efficient intracellular trafficking.^{8–11}

It has been recognized that the installation of targeting moieties on the surface of a gene delivery vector leads to more

Received: April 9, 2011

Accepted: August 4, 2011

Revised: July 27, 2011

Published: August 04, 2011

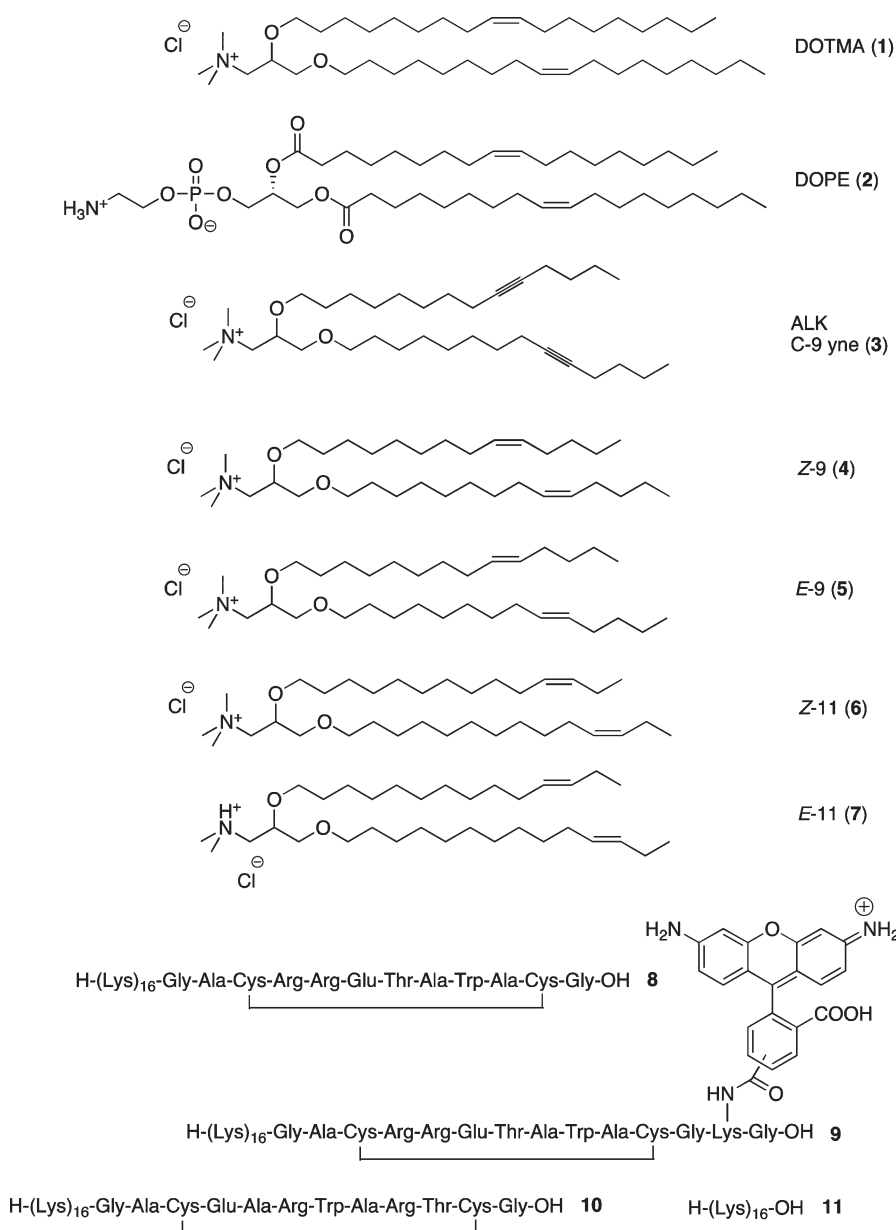


Figure 1. Structures of the lipids 1–7, peptide 8 and fluorescently labeled peptide 9, scrambled peptide 10 and K₁₆ peptide 11.

efficient internalization via receptor-mediated endocytosis, and consequently higher transfection efficiency. As a result, various ligands such as polysaccharides, antibodies and peptides have been incorporated into established nonviral delivery vectors in an attempt to improve their targeting, internalization, and transfection efficiency.^{8,9,12,13} For example, vectors prepared from polymers (known as polyplexes) containing cationic peptides rich in basic residues such as arginine, histidine or lysine are able to efficiently condense nucleic acid into small particles provided the peptide chain contains approximately 13 or more cationic residues.^{14–17} These peptide sequences have been combined with sequences from synthetic or virally derived peptides, designed variously to aid endosomal release, enhance nuclear localization, selectively target the vectors to specific cells via cell surface receptors, or a combination thereof.^{18–20} Of the numerous cell receptors that have been targeted, epidermal growth factor (EGF) receptors^{21,22} and integrins^{18,19} have been widely studied.

Combining these multifunctional peptides with cationic liposomes gives lipopolyplex delivery agents,^{8,9,12,13} which frequently have enhanced stability and transfection properties.^{23,24}

A synthetic gene delivery system has previously been described comprising a mixture of cationic lipid (L), an integrin-targeting peptide (P) and plasmid DNA (D) which, when combined electrostatically, forms LPD complexes with highly synergistic properties and transfection efficiencies that were orders of magnitudes higher than the equivalent lipid:DNA (LD) or peptide:DNA (PD) complexes.^{25–40} Significantly LPD complexes prepared using the lipids DOTMA (1) and DOPE (2) in a 1:1 weight ratio²⁵ and incorporating a targeting peptide were also able to transfect nondividing cells.²⁵ Furthermore the LPD complexes exhibited low toxicity and immunogenicity when examined in vitro and in vivo.^{26–29,33,35} Fluorescence quenching and fluorescence correlation spectroscopy (FCS) measurements have suggested that the structure of similar integrin targeting LPD vectors

possessed a tightly bound DNA–peptide core surrounded by a lipid layer from which (at least some of) the cyclic integrin domain protrudes.³¹

In the present study we have investigated and characterized the biophysical and biological behavior of LPD vectors prepared using a series of structurally related C-14 cationic lipids (3–7) (Figure 1) together with a bifunctional peptide (8) (Figure 1). These lipids have shown higher transfection efficiencies than their C-18 analogue, DOTMA, when formulated as LD complexes.³⁸

The peptide component, 8, of the LPD complexes investigated here was previously designed to both mediate the condensation of DNA and target cell surface receptors.³¹ The 16-lysine region mediates DNA binding, condensation and enzymatic protection capacity, and the cyclic region (CRRETAWAC) targets $\alpha_5\beta_1$ integrin cell surface receptors.⁴¹ As well as targeting integrin receptors, LPD vectors are thought to also be able to bind non-specifically to anionic proteoglycan cell-surface moieties due to their overall cationic nature.³⁰

As for the choice of lipids, previous studies using C12:1 to C18:1 analogues of DOTMA have shown that, when formulated with DOPE in LPD complexes,²⁸ C14:1 lipids with a cis double bond at C11 exhibited higher transfection levels in 1HAEO cells, when compared to the equivalent formulation containing DOTMA (C18). This result highlighted the potential advantages of using cationic lipids possessing shorter hydrophobic chains for gene delivery. We have therefore investigated the most promising C14 analogues of DOTMA incorporating an alkyne group at $\Delta 9$ and cis and trans moieties at $\Delta 9$ and $\Delta 11$ of the alkyl chain (lipids 3–7, Figure 1) in a 1:1 weight mixture with the helper lipid DOPE (2). In addition the cationic lipid DOTMA was also studied as a comparator. The biophysical properties and transfection efficiencies of these lipids and their respective lipid: DNA (LD) complexes were extensively studied in a previous publication.³⁸ Interestingly, despite the small structural changes between those lipids, highly significant changes in transfection efficiencies were observed which were attributed to the packing of lipid in the LD complex and its ability to interact with the DNA it encapsulates. The current study therefore focuses on using a range of biophysical techniques including dynamic light scattering, electron microscopy and small angle neutron scattering (SANS) to generate detailed information about the internal structure of the LPD complexes in the presence of the targeting peptide and to determine whether the structure of the LPD complexes formed by the various lipids is different. DNA binding and protection from enzymatic degradation was investigated by gel electrophoresis. Transfection, uptake and internalization studies of selectively fluorescently labeled components of the LPD vector were studied using confocal microscopy. Where appropriate, the results of the LPD complexes are compared to the corresponding LD or PD complexes.

2. MATERIALS

The lipids, Lipofectamine, DOTMA (*N*-[1-(2,3-dioleoyloxy)-propyl]-*N,N,N*-trimethylammonium chloride) and DOPE (dioleoylphosphatidylethanolamine) were purchased from Invitrogen Life technologies, U.K., TCI Europe N. V. Belgium, and Avanti Polar Lipids, USA, respectively. 2-(4,4-Difluoro-5-methyl-4-bora-3a,4a-diaza-s-indacene-3-dodecanoyl)-1-hexadecanoyl-*sn*-glycero-3-phosphocholine (β -BODIPY 500/510 C₁₂-HPC) (BODIPY-HPC), Rhodamine Green succinamidyl ester (mixture of 5- and 6-isomers) and OptiMEM were purchased from Invitrogen Molecular Probes, U.K. pETp450 plasmid (pDNA) purified

from an *Escherichia coli* JM109 transformed strain) was supplied from Institute Laue-Langevin (ILL), Grenoble, France, and was used only for the small angle neutron scattering studies. All other studies used the gWIZ-Luciferase plasmid (pDNA), obtained from Aldveron, USA, and which was labeled, where appropriate, with rhodamine using Label IT TM-Rhodamine Labeling Kit purchased from Mirus, USA. Calf thymus DNA (ctDNA) was purchased from Sigma, Pool, U.K. DAPI (4',6-Diamidino-2-phenylindole dihydrochloride) was purchased from Thermo Scientific, USA. GelRed was purchased from Gencompare, Belgium, and Luciferase assay kit was purchased from Promega, U.K. All other reagents were purchased from Sigma, Poole, U.K., unless otherwise stated. All reagents were of the highest grade possible and were used without further purification. Deionized water was used throughout the study.

3. METHODS

3.1. Synthesis. Chloride salts of lipids 3–7 were synthesized as previously described.³⁸ Peptides 8 (K₁₆GACRRETAWACG), its scrambled version 10 (K₁₆GACEARWARTCG and 11 (K₁₆) were synthesized on a MultiSynTech Syro peptide synthesizer using commercially available Fmoc amino acids (Novabiochem) and standard automated protocols. Once the linear peptides 8 and 10 had been assembled, disulfide bond formation was carried out on-resin⁴² as follows. To a sintered reaction vessel containing the solid support with the completed peptide sequence was manually added a solution of iodine (0.100 g) in DMF (1 mL), and the resulting mixture was agitated by vortex for 20 s with a 4 min break for a total of 4 h. Upon completion of the synthesis of 8, 10 and 11 on the synthesizer, the peptidyl-resin was washed thoroughly with DCM to remove traces of DMF; to the sintered vessel was added a cocktail solution of TFA/TIS/water (95:2.5:2.5, 2 mL), and the reaction was left to stand for at least 3 h. The resulting solution was removed from the vessel, and the resin was washed with neat TFA (2 \times 1 mL). The peptide was precipitated from cold Et₂O and isolated by centrifugation. The pellet was dissolved in water and freeze-dried to afford the crude peptide. The crude peptides were further purified by preparative reverse phase HPLC with aqueous TFA (0.1% v/v) and acetonitrile (with 0.1% TFA, v/v) using either a Supelco column (25 cm \times 21.2 mm) (for peptide 8) or a Phenomenex Onyx Monolithic Semi-Prep C18 column (100 \times 10 mm, flow rate 9.4 mL min⁻¹) (for peptide 10 and 11). The purified peptide 8 was then analyzed by analytical reverse phase chromatography using a Supelco column (25 cm \times 4.6 mm) with a 10 to 50% MeCN gradient run over 25 min: *t*_R 7.8 min. *m/z* (ES⁺), 1111.43 ([M + 3H]³⁺), 833.85 ([M + 4H]⁴⁺), 667.47 ([M + 5H]⁵⁺), 556.40 ([M + 6H]⁶⁺) for a mass of 3331.5. Peptides 10 and 11 were analyzed by analytical phase chromatography using a Phenomenex Onyx Monolithic C18 (100 \times 3 mm, flow rate 0.85 mL min⁻¹) column with a 10 to 90% MeCN run over 20 min. Peptide 10: *t*_R 8.6 min; *m/z* (ES⁺), 833.22 ([M + 4H]⁴⁺), 666.72 ([M + 5H]⁵⁺), 555.69 ([M + 6H]⁶⁺), 473.79 ([M + 7H]⁷⁺) for a mass of 3331.5. Peptide 11: *t*_R 5.2 min; *m/z* (MALDI-TOF) 2067.9 ([M + H]⁺), for a mass of 2067.2.

Peptide 9 (K₁₆GACRRETAWACGK*G), where K* indicates a Lys residue with Rhodamine Green attached to the ϵ -NH₂, was synthesized in a similar manner. Fmoc-Lys(ivDde)-OH was used for the Lys residue at position 29, and Boc-Lys(Boc)-OH was used at the N-terminus. After assembly of the linear sequence the ivDde group was removed by treatment with a hydrazine

monohydrate solution in DMF, followed by on-resin coupling with Rhodamine Green succinimidyl ester (mixture of isomers, 2 equiv) and DIPEA (4 equiv) with agitation by vortex for 20 s with a 4 min break for a total of 18 h. The peptidyl-resin was then washed with DMF (6×1 mL), followed by dichloromethane (6×1 mL), and cleaved from the solid support and worked up as described previously.³³ In order to form the disulfide bond, the lyophilized solid was dissolved in doubly distilled water (≤ 0.25 mg/mL) and stirred for 10 days. The peptide was purified by preparative reverse phase HPLC with aqueous TFA (0.1% v/v) and acetonitrile (with 0.1% TFA, v/v), with a gradient of 10 to 25% MeCN run over 25 min using a Supelco column ($25 \text{ cm} \times 21.2 \text{ mm}$). The purified peptide was analyzed by analytical HPLC using an Onyx monolithic C18 column (Phenomenex) ($100 \times 3.0 \text{ mm}$, flow rate of 0.85 mL/min) with a gradient of 5–90% MeCN (0.1% TFA) in H_2O (0.1% TFA) over 30 min: t_R 12.9 and 13.3 min (corresponding to the two isomers of Rhodamine Green); m/z (ES+) 968.62 ($[\text{M} + 4\text{H}]^{4+}$), 775.11 ($[\text{M} + 5\text{H}]^{5+}$), 646.09 ($[\text{M} + 6\text{H}]^{6+}$), 553.93 ($[\text{M} + 7\text{H}]^{7+}$) for a mass of 3871.

3.2. Preparation of Vesicles. Vesicles were prepared using the cationic lipids 1 and 3–7 at a 1:1 weight ratio with DOPE (2) at a total lipid concentration of 1 mg/mL or higher depending on the requirements of the particular experiment. For the purpose of fluorescence confocal microscopy experiments, 10% w/w of the DOPE lipid was replaced by BODIPY-HPC. All the vesicles were prepared using the thin film method, whereby the required amount of lipid, usually a mixture of 1 mg of cationic lipid and 1 mg of DOPE, were weighed into a round-bottom flask and dissolved in 5 mL of a 1:1 chloroform:methanol mixture. The solvent was evaporated in vacuo to produce a thin film of lipid, which was then rehydrated with 2 mL of ultrapure, double filtered water. The resulting crude vesicle suspension was then sonicated on ice for 10 min using a Lucas Dawes probe sonicator (model: 7535A) fitted with a tapered microtip operating at 50% of maximum output. The vesicles were centrifuged at 13,000 rpm ($\sim 16000g$) for 10 min to remove any titanium particles shed from the sonicator. For the purpose of SANS experiments D_2O was used instead of H_2O and the vesicles prepared at 2 mg/mL of total lipid.

3.3. Formulation of LD and LPD Complexes. LD complexes were formed by adding equal volumes of DNA, either ctDNA or pDNA, to the lipid vesicles to produce lipid:DNA weight ratios of 4:1, unless otherwise indicated. A weight ratio of 4:1 equates to an approximately 1:1 charge ratio for DOTMA containing LD complexes and a 1.1:1 charge ratio for LD complexes containing C14 lipids. In all experiments using pDNA, gWIZ-luc plasmid was used with the exception of the SANS measurements where the pET-p450 plasmid was used. The samples were mixed by hand shaking and left to complex for 15 min at room temperature before further use. The final concentration of DNA used depended on the experiment performed.

LPD complexes were prepared at lipid:peptide:DNA weight ratios of 2:2:1 or 2:4:1 (using either ctDNA or pDNA), which equates to charge ratios of approximately 1:6:2 and 1:12:2, respectively. In preliminary experiments the order of mixing of the three components was shown to play a crucial role in the transfection efficiency of the resulting LPD complex. Maximum transfection efficacy was observed (data not shown) when the LPD complexes were prepared by first adding a solution of peptide 8 to a suspension of lipid vesicles, followed by the addition of a solution of DNA with gentle mixing. As a consequence all experiments reported in this paper were prepared using the same

order of mixing. Note that the concentrations of the three individual solutions used were adjusted so that volume ratios of 1:4:5 (lipid:peptide:DNA) were used to prepare the LPD complexes.

3.4. Dynamic Light Scattering. The apparent hydrodynamic size and polydispersity of the vesicles and complexes together with their zeta potentials were measured by dynamic light scattering using either a Brookhaven Zeta-Plus particle sizer, Brookhaven Instruments, USA, or a Malvern Zetasizer Nano ZS, Malvern U.K. The latter instrument was used when only low concentrations and volumes of a sample were available. When using the Brookhaven Zeta Plus, vesicles of lipid concentration of 0.05 mg/mL, and LD and LPD complexes containing 0.125 mg/mL of DNA were measured. In contrast, when using the Malvern Zetasizer Nano ZS, vesicles containing 0.01 mg/mL of lipid and LD and LPD complexes containing 2.5–5 μg /mL of DNA were determined. With both instruments only one scattering angle (90° and 173° for the Brookhaven and Malvern respectively) was used to measure particle size. The quoted apparent hydrodynamic size is that of the equivalent spherical particle determined using cumulants analysis. In order to get as accurate an assessment of hydrodynamic size as possible in all cases, samples were measured at a sufficiently low concentration to ensure the absence of any interparticulate interactions. Although the samples prepared for the SANS experiments were dispersed in D_2O and not H_2O , they were either diluted in H_2O prior to size measurement (vesicles), so that the small amount of D_2O present did not affect the measurement of size, or alternately measured in D_2O where the viscosity used to determine particle size was that of D_2O .

3.5. Gel Retardation and Protection Assay. The pDNA binding efficiency of LD, PD and LPD complexes was determined using agarose gel electrophoresis. Samples were prepared so that the final pDNA concentration was 1 μg per 10 μL per well and formulated at weight ratios of 4:1 and 8:1 for LD complexes, 2:1 and 4:1 for LP complexes and 2:2:1 and 2:4:1 for LPD complexes and prepared as described in section 3.3. To each 10 μL of sample, 2 μL of gel loading buffer (prepared using 0.25% w/v bromophenol blue in a 40% w/v sucrose solution) was added before loading the sample onto the gel.

DNA release and protection from enzymatic degradation was also tested. To identical samples as described above, 1 μL of 0.1 M magnesium chloride was added followed by 1 μL of 1000 U/mL DNase I. The mixture was incubated at 37°C for 10 min, after which the enzyme was deactivated through the addition of 2.5 μL of 0.5 M EDTA. 1.25 μL of 10 mg/mL poly aspartic acid (pAsp) was then added to release any protected DNA in order to detect it on the gel. Complexes were also treated with pAsp in the absence of DNase I to test the efficiency of DNA release from the complexes. Free pDNA and pDNA treated with DNase I were also used as positive and negative controls respectively. 3 μL of gel loading buffer was added to the samples, which were then loaded into a 0.8% w/v agarose gel containing GelRed in Tris-acetate-EDTA (TAE) buffer at pH 7.4 and run at 80 mV for one hour. The gel was visualized using a Herolab EASY UV transilluminator.

3.6. Transmission Electron Microscopy. LD and LPD complexes, prepared as described in section 3.3 at weight ratios of 4:1 and 2:4:1 respectively and at a final pDNA concentration of 0.01 mg/mL, were prepared for transmission electron microscopy by placing a drop of sample on a Formvar 200 mesh copper grid for 1 min, after which time the grid was dried using a filter paper wick. Next the grid was placed on a drop of a 4% w/v uranyl acetate solution for ~ 5 min, after which time the grid was washed first with 50% ethanol and then in water and dried. The samples

were visualized using an FEI Tecnai T12 transmission electron microscope, USA

3.7. Small Angle Neutron Scattering (SANS). SANS measurements were performed on the LOQ beamline at the ISIS pulsed neutron source (CCLRC Rutherford-Appleton Laboratory, Didcot, U.K.). All samples were prepared fresh in deuterium oxide (D_2O) and then diluted and mixed according to section 3.3 to produce total lipid concentrations of 1 mg/mL for the vesicular samples, and a DNA concentration of 0.125 mg/mL for the LD and LPD complexes. Since 4:1 and 2:4:1 weight ratios were used for the LD and LPD samples, the final concentration of lipid in each sample was 0.5 mg/mL and 0.25 mg/mL respectively. Additionally samples containing peptide 8:lipid at 2:1 weight ratios were prepared at final concentrations of 1 mg/mL peptide 8 and 0.5 mg/mL lipid. Note that the vesicles were prepared using 5 min probe sonication, instead of the 10 min used throughout the rest of the paper. The only detectable difference the length of sonication makes is to the initial size of vesicles. Either ctDNA or pDNA (pET-p450) was used in the SANS study. Samples were placed in cleaned disk-shaped fused silica cells of 2 mm path length and measured at 25 °C. The scattering intensity, $I(Q)$, of a sample as a function of the scattering vector, $Q = (4\pi/\lambda) \sin(\theta/2)$ (where $\theta/2$ is the scattering angle), was corrected for the appropriate sample transmission. Backgrounds from pure D_2O were subtracted as appropriate, and all fitting procedures included flat background corrections to allow for any mismatch in the incoherent and inelastic scattering between the sample and solvents. Fitted background levels were always checked to ensure that they were of a physically reasonable magnitude. The SANS data for the vesicles alone, vesicles mixed with peptide 8, LD and LPD complexes were modeled assuming (isolated) infinite planar (lamellar) sheets as well as one-dimensional paracrystals (stacks) to account for the presence of any multilamellar vesicles.⁴³

When modeling the vesicles as (single) sheets, the fits to the SANS data were obtained by the least-squares refinement of three parameters, namely, L , $R\sigma$ and the absolute scale factor (together with the background, as described above), where $R\sigma$ is the Lorentz correction factor which provides some information about the extent of rigidity or curvature of the lamellar sheets. Since the polydispersity on the bilayer thickness ($\sigma(L)/L$) can only reliably be fitted if good quality data are available in the high Q regime, and given the limited Q range of the measurements recorded here, this parameter was fixed as 0.0001, i.e. effectively zero, for all the systems studied. In the mixed sheet and stack model, the fits to the SANS data were obtained by least-squares refinement of seven parameters, namely, the mean bilayer thickness (L), the Lorentz factor ($R\sigma$), the number of bilayers in the stack (M), their mean separation (D), the width of the Gaussian distribution in the plane $\sigma[(D)/D]$ and the absolute scale factors for the unilamellar and multilamellar vesicles. The polydispersity on the bilayer thickness ($\sigma(L)/L$) was again fixed as 0.0001, while the polydispersity of the d -spacing was fixed 0.05. Furthermore when modeling a mixed population of sheets and stack, L , $\sigma(L)/L$, and $R\sigma$ were constrained to be the same values for both the isolated sheets and stacked lamellae, a not unreasonable assumption. In the present study fitted value of $R\sigma$ was in the range of 250 ± 20 unless otherwise stated. As in our previous paper³⁸ the SANS data obtained for the LD complexes were modeled using the stack model and with an extra term to account for low Q scattering that varied with a -4 gradient. A gradient of -4 is suggestive of “Porod scattering”, and is characteristic of

scattering from smooth interfaces of large particles of uniform scattering length density. For all models, the least-squares refinements were performed using the model-fitting routines provided in the FISH software.⁴⁴

3.8. Cell Culture. MDA-MB-231 breast cancer cells were a gift from the Randall Division of Cell and Molecular Biophysics, King's College London. The cells were cultured in Dulbecco's modified Eagle's medium (DMEM), supplemented with 10% v/v fetal bovine serum (FBS), 1% v/v L-glutamine 200 mM, 1% v/v MEM-nonessential amino acids (NEAA) and 0.5% v/v gentamicin solution at 37 °C, 5% CO_2 and 90% relative humidity. The cells were fed every other day and passaged every 3–4 days, when at ~70–80% confluency, using 0.25% w/v trypsin–EDTA solution.

3.9. Transfection Experiments. MDA-MB 231 cells were plated on 24-well plates at 1×10^5 cells per well and incubated at 37 °C, 5% CO_2 and 90% relative humidity for 24 h. On the day of the experiment, DMEM growth medium was removed from each well, the cells rinsed once with 200 μ L of PBS, and then 200 μ L of OptiMEM was added. 200 μ L of either LD or LPD complex was added so that the final pDNA concentration was 1 μ g per 400 μ L per well, $n = 4$. All complexes were prepared at 4 times concentration, and diluted first 1:1 v:v with OptiMEM, followed by a further 1:1 dilution upon addition to the cells (200 μ L of the complex solution was added to wells containing 200 μ L of OptiMEM). The LD complexes were prepared by mixing equal volumes, usually 200 μ L, of the required vesicle suspension with 200 μ L of a 0.02 mg/mL pDNA solution. The mixtures were left to complex for 15 min at room temperature, then diluted to 800 μ L with OptiMEM. 200 μ L from the above mixtures were added to each of four wells containing 200 μ L of OptiMEM producing a final DNA concentration of 1 μ g per well.

LPD complexes of 2:2:1 and 2:4:1 weight ratios were prepared by first adding 160 μ L of an either 0.05 or 0.1 mg/mL solution of peptide (0.1 or 0.07 mg/mL solution in the case of peptide 11 to achieve a 2:4:1 or 2:2.8:1 weight ratio, the latter of which equates to 1:12:2 charge ratio, which is equivalent to that produced by mixing a 2:4:1 weight ratio with peptide 8) to 40 μ L of a 0.2 mg/mL of vesicle suspension, followed by the addition of 200 μ L of 0.02 mg/mL pDNA to the lipid:peptide mixture. The samples were mixed, kept at room temperature for 1 h and diluted in OptiMEM to a final volume of 800 μ L. 200 μ L of the complex solution were transferred to each of four wells containing 200 μ L of OptiMEM. Lipofectamine:pDNA complex, prepared at a 4:1 weight ratio was used as a positive control.

The plates were incubated at 37 °C for 4 h, after which time the cells were washed once with PBS buffer and replaced with serum supplemented DMEM culture medium and incubated for 48 h, to allow for luciferase expression, which was measured using a luciferase assay kit according to the manufacturer's protocols. The luciferase activity of the lysate was measured by transferring 20 μ L of the lysate to a well in a white 96-well plate and measuring the sample for 10 s using an MLX Microtiter Plate Luminometer (Dynex Technologies, Chantilly, USA) with an automatic feeding system delivering 100 μ L of the reconstituted luciferase assay reagent into each well. The amount of protein in each transfection lysate was measured using a Bio-Rad (Hercules, CA, USA) RC-DC protein assay according to the manufacturer's instructions. Luciferase activity was expressed as relative light units (RLU) per milligram of protein (RLU/mg protein).

3.10. Confocal Fluorescence Internalization Studies. MDA-MB-231 cells were transfected with LD or LPD complexes

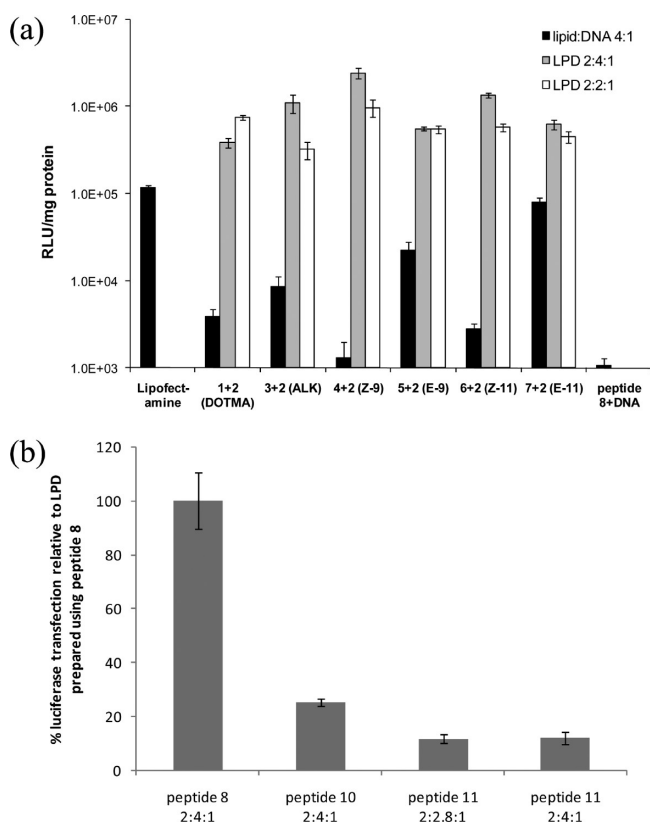


Figure 2. (a) Transfection efficiency of the C14 lipids and DOTMA in the presence and absence of peptide 8 in MDA-MB 231 cells. In addition the results for Lipofectamine and peptide 8:DNA at 4:1 weight ratio are also shown. Black bars: lipid:DNA 4:1 weight ratio. Gray bars: lipid: peptide 8:DNA 2:4:1 weight ratio. White bars: lipid:peptide 8:DNA 2:2:1 weight ratio. (b) % transfection efficiency of LPD complexes prepared using lipids 1:2 (DOTMA:DOPE) with either targeting peptide 8 (denoted as 100% transfection), its scrambled version (peptide 10), both at 2:4:1 weight ratio, or the K₁₆ DNA binding peptide (peptide 11) at 2:2.8:1 and 2:4:1 weight ratios (the former of which corresponds to 1:12:2 charge ratio, which is equivalent to that produced by mixing a 2:4:1 weight ratio when using peptide 8 or 10) ($n = 4 \pm$ standard deviation).

in 24-well plates fitted with sterilized 13 mm circular coverslips (purchased from Agar Scientific, U.K.) as described in section 3.9 with the exception of using various combinations of fluorescently labeled lipid, pDNA or Rhodamine Green-labeled peptide 9. Lipids were labeled by incorporating 10% w/w of (green) BODIPY-labeled HPC lipid into the lipid film during vesicle formation. gWIZ-luc plasmid was labeled with (red) rhodamine using a Label IT™-Rhodamine Labeling Kit according to the manufacturer's protocol. 100% of the labeled plasmid and peptide 9 were used.

After a 4 h incubation, the complexes were removed and the cells washed once with PBS buffer before fixation or further incubation with supplemented cell culture medium. The cells were fixed with 4% w/v paraformaldehyde in PBS for 20 min at time intervals of 0, 4, and 10 h after the initial 4 h incubation. Cells were then permeabilized with 0.2% v/v Triton X-100 solution for 20 min followed by treatment with 1 mg/mL sodium borohydride in PBS for 5 min to quench aldehyde groups. The cell nucleus was stained blue by adding 1 μ g/mL of DAPI solution in PBS for 2 min followed by extensive washing with PBS. Washed coverslips were mounted onto microscope slides using

Mowiol 4-88 mounting media containing 2.5% w/v DABCO as an antifade agent. Confocal fluorescence images were acquired on a confocal fluorescence laser-scanning microscope (model LSM 510; Carl Zeiss Inc.) equipped with 40 \times /1.3Plan-Neofluar and 63 \times /1.4Plan-APOCHROMAT oil immersion objectives, or a Leica DMIRE2 (Leica Microsystems, Germany).

4. RESULTS

4.1. In Vitro Transfection. The results of experiments determining the transfection ability of the LPD complexes (containing the gWIZ-luc plasmid) in MDA-MB 231 breast cancer cells are shown in Figure 2. For comparison the transfection results obtained with LD complexes prepared at a lipid:pDNA weight ratio of 4:1 in the absence of peptide 8 and tested at the same time are also given. LD complexes of this composition were selected for study as this ratio of lipid:pDNA yielded the highest level of transfection in our earlier studies.³⁸ The results obtained for the LD complexes in this study (Figure 2a) are very similar to those reported in ref 38, which were obtained on a separate occasion. As can be seen the LD complexes exhibited similar or lower levels of transfection efficiency to that obtained with the gold standard, Lipofectamine.

When considering the transfection efficiencies obtained, noticeable trends were observed in the transfection efficiency with structure. Generally LD complexes prepared from the trans lipids, 5 and 7, resulted in higher transfection efficiencies than the LD complexes containing the cis lipids, 4 and 6. Furthermore, complexes containing lipids with the double bond at position C-11 were more efficient than those where the double bond was positioned at C-9. Therefore complexes containing E-11 (7) demonstrated the highest transfection efficiency of any of the LD complexes tested, a level comparable to that of Lipofectamine. Similar trends in efficiency with lipid structure were observed in the human alveolar epithelial cell line, 1HAEO.³⁸

In the case of the LPD complexes, it appears that the dominant influence on transfection efficiency is the targeting peptide (8), the presence of which greatly increases the transfection efficiency of the lipids at both the 2:2:1 and 2:4:1 LPD weight ratios when compared to the LD complexes. In fact increases in transfection of up to 2500-fold were obtained in the case of LPD complexes containing lipid 4 compared to that seen with the equivalent LD complex. This increase in transfection is thought to be attributable to a synergistic activity between the lipids and the peptide, since complexes prepared from peptide:pDNA at a 4:1 weight ratio showed negligible transfection. In addition LPD complexes prepared using the higher amount of peptide, i.e. the 2:4:1 weight ratio complexes, tended to transfect better than those made using the lower peptide weight ratio of 2:2:1, with the exception of LPD complexes containing DOTMA, where the 2:2:1 weight ratio complex transfected slightly more effectively, and the LPD complexes containing 5, where the amount of peptide had no obvious effect on the level of transfection. LPD complexes containing either 3, 4 or 6 at a lipid:peptide:pDNA weight ratio of 2:4:1 exhibited the highest levels of transfection.

In addition to the above-mentioned synergistic effect between the peptide and the lipid, the presence of the targeting sequence CRRETAWAC was also shown to offer targeting selectivity toward the MDA-MB 231 breast cancer cells since transfection using LPD complexes prepared using lipid 1:2 with a peptide containing a scrambled targeting sequence (peptide 10) and a K₁₆ DNA binding peptide in the absence of any targeting sequence

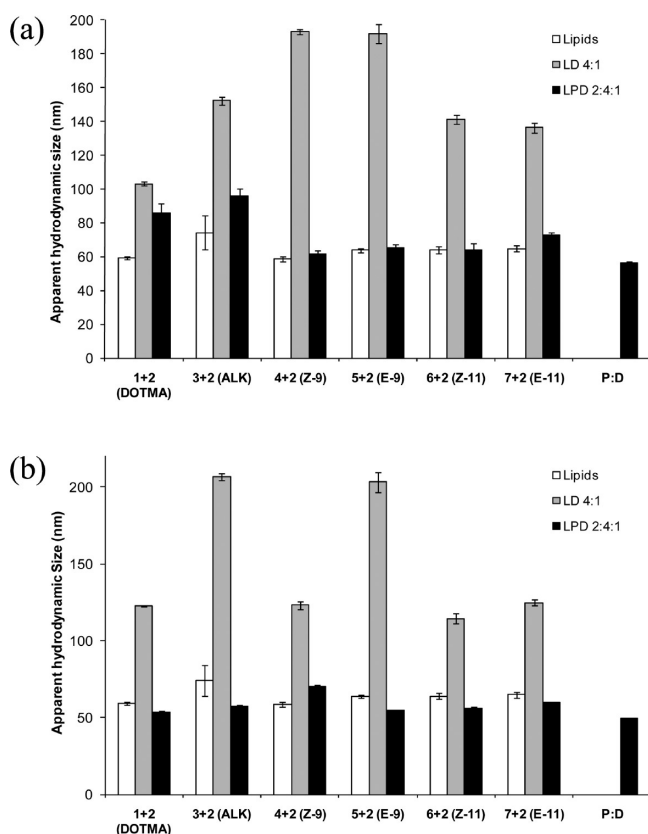


Figure 3. The apparent hydrodynamic size of (white bars) vesicles composed of cationic lipid + 2, (grey bars) LD complexes prepared at a 4:1 weight ratio and (black bars) LPD complexes prepared with peptide 8 at a 2:4:1 weight ratio using (a) ctDNA and (b) pDNA ($n = 5 \pm$ standard deviation).

(peptide 11) only showed 25% and 12% transfection respectively, when compared to LPDs containing peptide 8 when tested at the same charge ratios of 1:12:2 (equivalent to 2:4:1 weight ratios using peptides 8 and 10, and 2:2.8:1 using peptide 11). Furthermore, a 2:4:1 weight ratio comparison using peptide 11 showed the same transfection efficiency as that produced by the 2:2.8:1 weight ratio as shown in Figure 2b. This indicates that the high transfection efficiency seen with the LPD complexes prepared with peptide 8 is at least partially a consequence of the targeting sequence.

Interestingly, as shown in Figure 2a, although there appeared to be less of an effect of lipid structure on transfection efficiency when the lipid was formulated as an LPD complex, compared to when it was formulated as an LD complex, the chemical structure of the constituent lipids still influenced the level of transfection obtained. However, for LPD complexes the opposite trend to that seen in LD complexes was observed. Notably, the *cis* lipids, 4 and 6, exhibited superior transfection efficiencies compared to those containing the *trans* lipids, 5 and 7. Although the LPD complexes prepared with the Z-9 (4) lipid tended to exhibit a greater transfection than the corresponding complexes containing the Z-11 lipid (6), there was little difference in the transfection efficiency obtained for the two *trans* lipids. Significantly, the level of transfection obtained with the 2:4:1 weight ratio LPD complexes was up to 20 times higher than that of Lipofectamine, and 6 times higher than that of DOTMA (1) in the 2:4:1 LPD complex. This marked improvement in transfection in going

from C18 chain lengths in DOTMA to C14 is extremely interesting and highlights how modification of lipid chain lengths used in LPD systems can be tailored for enhanced performance.

In order to understand the reason for the differences observed in transfection efficiency between the two types of complexes, and between the various types of lipid, a range of biophysical techniques including dynamic light scattering, small angle neutron scattering (SANS), gel electrophoresis and electron microscopy were employed to relate differences in internal structure and/or morphology of the complexes to transfection efficiency. In addition, the intracellular localization, fate and trafficking of fluorescently labeled complexes were studied by confocal fluorescence microscopy. Most of the studies reported below utilized LPD complexes prepared using the various lipids with peptide 8 (or peptide 9 for fluorescence confocal studies) at a 2:4:1 weight ratio and LD complexes prepared from a 4:1 weight ratio as these complexes exhibited the highest transfection efficiency of their type.

4.2. Size Analysis. The apparent hydrodynamic size of the vesicles, LD and LPD complexes formulated using the cationic lipids in combination with a 1:1 weight ratio of DOPE (2) and either ctDNA or pDNA at a DNA concentration of 2.5–5 $\mu\text{g/mL}$ is shown in Figure 3. (The sizing results obtained for the LD and LPD complexes prepared using higher concentrations of up to 0.1 mg/mL ctDNA are given in Figure 1 in the Supporting Information.) Regardless of the lipid used, after 10 min sonication all the vesicles exhibited a hydrodynamic size in the approximate size range 60–75 nm and polydispersities in the range 0.2–0.3. The small size suggests the presence of a population of predominately small unilamellar vesicles in suspension. It should be noted that there was very little difference in the apparent hydrodynamic size of the vesicles, recorded by dynamic light scattering over the range of lipid concentrations (0.01–0.05 mg/mL) used in the present study. Furthermore, the results of the sizing study were as expected, as it has been well established that a mixture of lipids 1 + 2 forms stable vesicles at room temperature.⁴⁵ In addition our previous biophysical studies have shown that the C14 lipids in the presence of 2 formed small vesicles, predominately unilamellar in nature.³⁸ The slightly smaller apparent hydrodynamic size of vesicle obtained in the present study is due to the longer sonication time, 10 min as opposed to the 5 min previously used.³⁸ As expected zeta potential measurements show that the vesicles all possess a positive charge (Table 1), explaining their high stability as regards size.

The addition to the vesicle suspensions of either ctDNA or pDNA at a final lipid:DNA weight ratio of 4:1 resulted in an increase in the apparent hydrodynamic size of the aggregates to a maximum of around 200 nm and polydispersity of 0.1–0.3, a result in line with that previously reported by us.³⁸ Interestingly the slightly smaller size of vesicles used in the present study made no difference to the size of the resultant LD complexes. Although the LD complex prepared at the 4:1 weight ratio is theoretically of neutral charge, zeta potential measurements in Table 1 showed that all the LD complexes possessed a *negative* charge, regardless of the particular lipid and type of DNA used to prepare the complex. Earlier studies³⁸ on LD complexes prepared at a range of lipid:DNA weight ratios suggested that a weight ratio of between 8:1 and 16:1 was required for LD neutrality since all the complexes prepared at the 16:1 weight ratio were positive. This result implies that more cationic lipid is required to completely neutralize the negative charge of the DNA than theoretically calculated.

Table 1. Zeta Potential (mV) of Cationic Lipid:2 Vesicles, LD and LPD Complexes Containing ctDNA or pDNA and Prepared at 4:1 and 2:4:1 Weight Ratios, Respectively ($n = 5 \pm$ Standard Deviation)^a

lipids	vesicles alone	LD 4:1		LPD 2:4:1	
		ctDNA	pDNA	ctDNA	pDNA
1 + 2	65.1 \pm 0.8	-17.5 \pm 0.9	-34.4 \pm 0.5	30.2 \pm 3.5	56.1 \pm 1.9
3 + 2	57.2 \pm 2.9	-7.3 \pm 0.3	-43.1 \pm 1.1	31.0 \pm 0.7	47.0 \pm 2.8
4 + 2	65.7 \pm 5.4	-18.4 \pm 0.2	-36.2 \pm 1.2	48.4 \pm 1.1	52.1 \pm 3.5
5 + 2	55.7 \pm 3.7	-31.5 \pm 1.1	-21.7 \pm 1.4	33.0 \pm 0.3	52.0 \pm 2.0
6 + 2	68.2 \pm 0.9	-24.0 \pm 0.9	-48.3 \pm 0.3	45.6 \pm 0.6	47.2 \pm 0.8
7 + 2	46.8 \pm 1.9	-29.5 \pm 0.3	-36.5 \pm 0.6	36.9 \pm 2.5	56.5 \pm 2.3

^aZeta potentials of the complexes prepared from peptide 8:ctDNA and pDNA at a weight mixing ratio of 4:1 were 41.4 \pm 0.8 mV and 32.1 \pm 2.6 mV respectively.

From Figure 3, it is clear that the apparent hydrodynamic size of the LPD complexes prepared at 2:4:1 weight ratio was significantly smaller than that of the LD complexes, and was much more similar in size to the original vesicles used to prepare the complexes, being in the approximate size range of 60–95 nm and with polydispersities in the range 0.2–0.3 for the LPD complexes containing ctDNA and 55–70 nm and with polydispersities of between 0.05 and 0.3 for those containing pDNA. Figure 3 also gives the size of the complexes formed between peptide 8 and DNA, which were slightly smaller than LPD complexes, at approximately 50 and 55 nm in the case of pDNA and ctDNA respectively.

It should be noted, however, that the sizes of the LD complexes and, to a slightly lesser extent, the LPD complexes were concentration dependent. Note that the concentrations of the samples whose apparent hydrodynamic size and zeta potential are displayed in Figure 3 and Table 1, respectively, were similar to those used in the transfection experiments, namely, 2.5–5 μ g of DNA per mL. When higher concentrations of up to 0.1 mg/mL ctDNA were used to prepare the complexes, slightly larger apparent hydrodynamic sizes of 200–250 and 150–190 nm were recorded for the LD complexes³⁸ and LPD complexes (see Figure 1 in the Supporting Information), respectively.

Despite the lower amount of lipid used to prepare the LPD complexes than the LD complexes, the presence of positively charged peptide meant that the total positive:negative charge ratio was 7:2 or 13:2 in the case of the LPD complexes as opposed to 1.1:1 in the case of the LD complexes. As a consequence, the zeta potential of all the LPD complexes was highly positive at \sim 30–50 mV for ctDNA containing complexes and \sim 45–55 mV for pDNA containing complexes, although lower than that obtained for the vesicles alone. As seen with the vesicles, the high positive charge displayed by the LPD complexes explains their high size stability.

4.3. Transmission Electron Microscopy. LD and LPD complexes prepared at 4:1 and 2:4:1 weight ratios, respectively, were visualized via transmission electron microscopy (TEM) using negative staining with uranyl acetate. Figure 4 shows images of the LD and LPD complexes formed by the E- and Z-lipids and containing pDNA. LD and LPD complexes prepared using lipids 1 and 3 in combination with 2 produced similar results (see Figure 2 in the Supporting Information). As can be seen, the presence of peptide 8 resulted in a considerable difference in the

size, structure and morphology of the complex compared to that prepared in its absence. In contrast to the large, irregular-shaped aggregates observed for the LD complexes, the LPD complexes were much smaller (around 50–100 nm in diameter) and predominately spherical in shape, although some rod-shaped structures were also visible in all LPD samples. The LPD complexes were all densely stained and did not seem to contain any visible internal structure when visualized at the higher magnifications in Figure 4d,h.

The LD complexes, in comparison, were much larger in size and contained distinct, repeating structures, which are thought to consist of strands of DNA sandwiched between bilayers of the cationic lipid and DOPE.^{7,38} Significantly in no case was there any noticeable difference in the structure of the LD or LPD complexes prepared from the different lipids and with pDNA (Figure 4) or ctDNA (data not shown). The results of the electron microscopy study agree with the light scattering studies in that the size of the LD complexes was much larger than that of the LPD complexes. Both types of complexes were polydisperse in nature when examined by TEM.

Figure 4i also shows a TEM of the complex formed from peptide 8 and pDNA at a 4:1 weight ratio (i.e., the same ratio as used for the LPD complexes shown in Figure 4). As can be seen, although these complexes were predominately rod-shaped in structure, some spherical particles were also observed with sizes of \sim 40–50 nm. It is worth commenting that the apparent hydrodynamic sizes measured for the peptide:pDNA complexes recorded using dynamic light scattering are an average of the particle ensemble assuming the presence of spherical particles and so it is not possible to *directly* compare the sizes obtained by dynamic light scattering with those determined by transmission electron microscopy, which is a number average technique and thus for polydisperse samples would be expected to yield a smaller average size than that obtained using dynamic light scattering which yields a volume average size of the hydrated complexes.

4.4. Small Angle Neutron Scattering (SANS). The variation in the intensity of the SANS as a function of Q is shown in Figure 5a for vesicles prepared using lipids 4 and 2 and in Figure 5c for LPD complexes containing lipid 4. It should be noted that the vesicles were those actually used to prepare the LPD complexes. For the purposes of comparison, the SANS data obtained for the corresponding LD complex, prepared using lipids 4 and 2, are shown in Figure 5b. Note that the SANS experiments reported here were obtained using pET-p450 plasmid, although we have previously reported no significant difference in the detailed molecular structure as determined by SANS of LD complexes prepared using ctDNA and this particular type of pDNA.³⁸ Figure 5d also shows the scattering curve obtained after vesicles prepared from lipids 4 and 2 had been added to peptide 8. This sample was of interest as all the LPD complexes prepared in the present study were made by adding (the cationic) peptide 8 to preformed (cationic) vesicles prior to the addition of the negatively charged DNA. Although not shown here, qualitatively similar variations in the SANS as a function of Q were observed for the corresponding samples prepared using the other lipids studied here (data not shown). It is clear from Figure 5 that the scattering pattern recorded for the LD complexes is very different from that reported for the vesicles, both in the presence and in the absence of peptide, as well as the LPD complexes, all of which look qualitatively very similar.

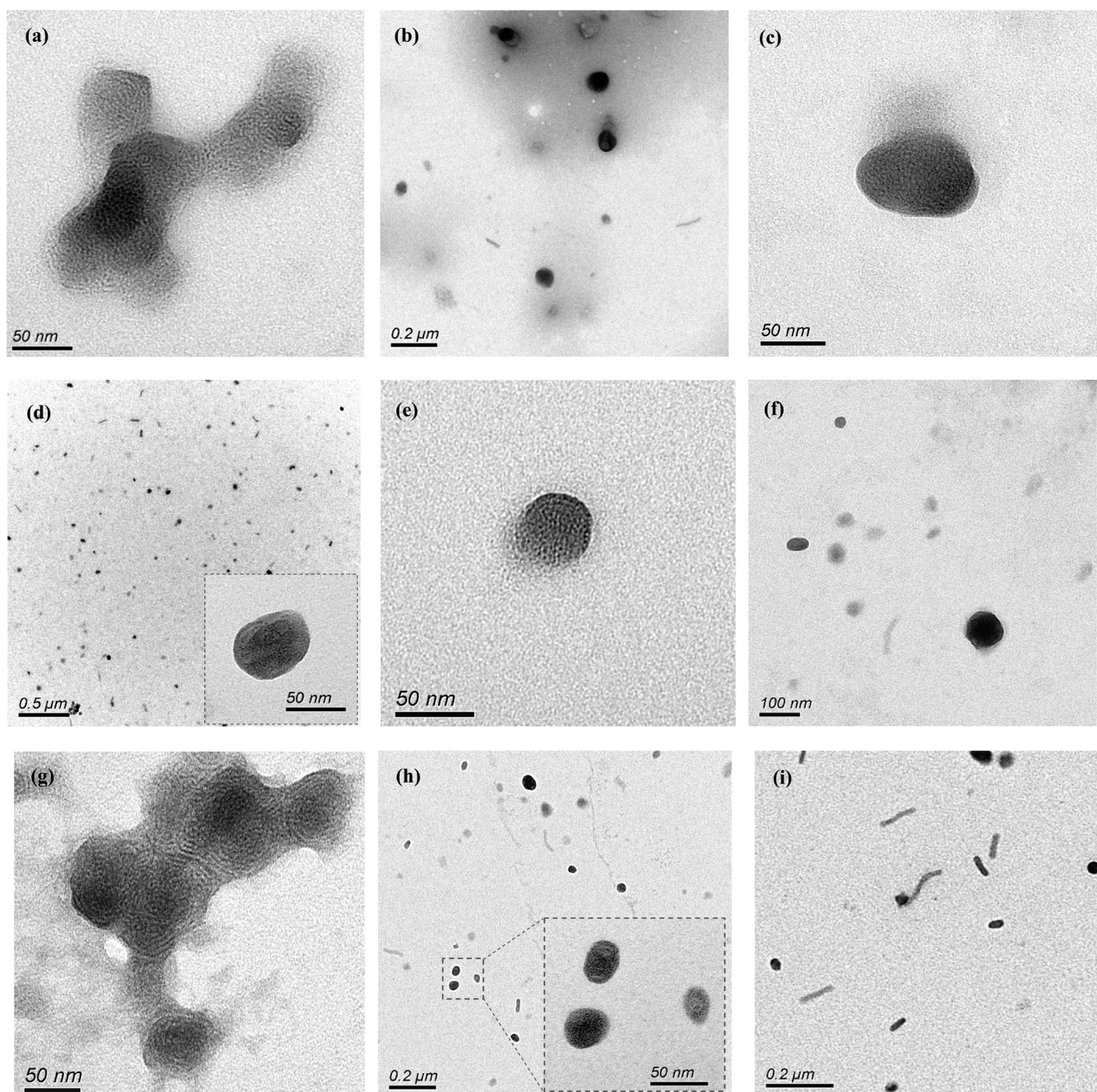


Figure 4. Transmission electron microscopy of LD complexes prepared at a 4:1 weight ratio using pDNA and lipid (a) 4:2, (c) 5:2, (e) 6:2 and (g) 7:2; LPD complexes prepared at a 2:4:1 weight ratio using peptide 8, pDNA and lipid (b) 4:2, (d) 5:2, (f) 6:2 and (h) 7:2; and peptide 8:pDNA complexes (i) prepared at a 4:1 weight ratio. All lipids were formulated at a 1:1 weight ratio with 2 and prepared at a concentration of 0.01 mg/mL of pDNA per sample.

The results of the analysis of the SANS data of the vesicles prepared by the cationic lipid and 2 have been previously reported³⁸ as has the analysis of the SANS data obtained for the LD complexes and are reproduced here for ease of discussion (Table 2). As recorded, the SANS data for the 2-containing cationic vesicles were well fitted using a model comprising a mixture of single, infinite planar (bilayer) sheets and one-dimensional paracrystals (stacks) as shown in Figure 6. The sizes of the vesicles were sufficiently large that, for the purpose of analyzing the SANS data obtained here, they could not be considered as hollow spheres (with the wall of the sphere

representing the lipid bilayer) but were considered rather as single, flat sheets (in the case of unilamellar vesicles) or stacks (in the case of multilamellar vesicles). Modeling of the SANS data suggested that the vesicles were predominantly unilamellar in nature, with only a very small number of multilamellar vesicles. This result is in agreement with the small size of the vesicles measured using dynamic light scattering, which indicates that only a small number of multilamellar vesicles, if any, were present.

In contrast, the SANS data recorded for the LD complexes could not be modeled using the same mixed model of single lipid

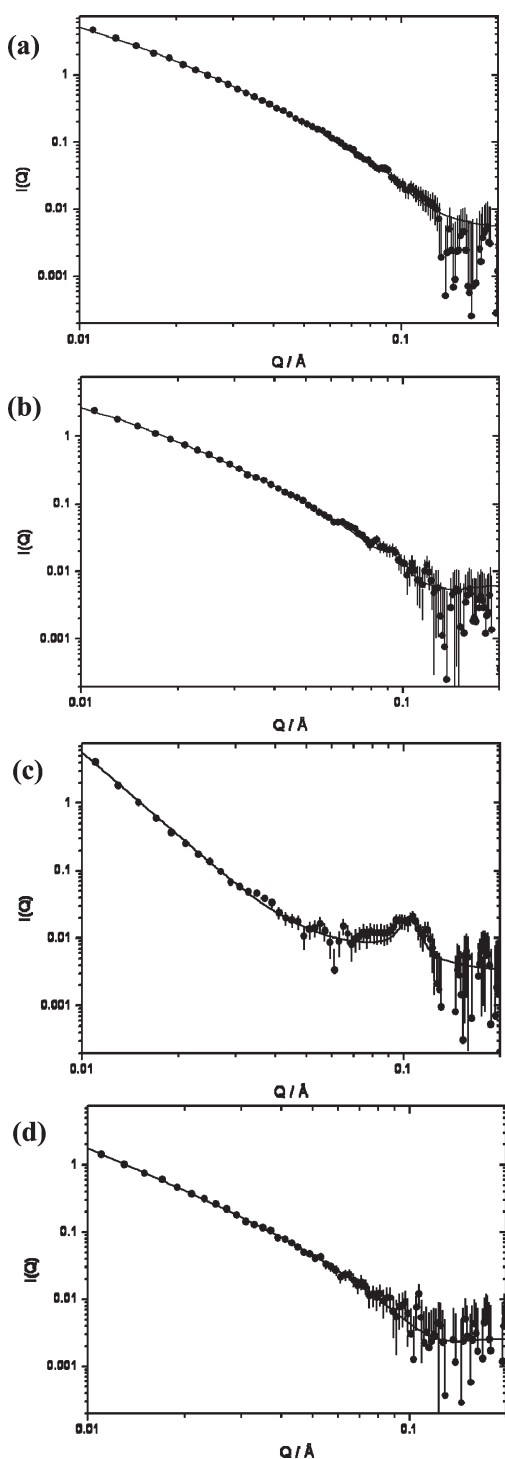


Figure 5. Small angle neutron scattering data (dots) at 298 K and the best fit to the data (solid line) for (a) vesicles of 4 containing 50 wt % 2 at a total lipid concentration of 1 mg/mL; (b) vesicles of 4:2 mixed with peptide 8 at a 1:2 lipid:peptide weight ratio, at 0.5 mg/mL lipid concentration; (c) LD complexes prepared from vesicles of 4:2 with pDNA at 4:1 lipid:DNA weight ratio containing 0.5 mg/mL of lipid; and (d) LPD complexes prepared from vesicles of 4:2 mixed with peptide 8 and pDNA containing 0.25 mg/mL of lipid. The best fit to SANS data shown in panels a, b and d was obtained using the mixed sheet and stack model while the best fit to the SANS data shown in panel c was using the stack model.

bilayers and stacks of similar bilayers as the vesicles but rather were well modeled as a preparation containing *only* multilamellar

Table 2. Structural Parameters Obtained for Cationic Vesicles Containing 2 and LD Complexes Formed Therefrom with pDNA at a Lipid:DNA Weight Ratio of 4:1 (Derived from FISH Modeling of the SANS Data) Measured at 298 K^a

lipids used	thickness (nm) and number of layers		<i>d</i> -spacing (nm)	
	vesicles	LD	vesicles	LD
1:2	4.47 (0.07) 2.0	4.54 (0.09) 56.0	6.50 (0.03) 6.18 (0.08)	
3:2	4.49 (0.07) 2.0	4.12 (0.10) 56.0	6.48 (0.01) 5.71 (0.08)	
4:2	4.46 (0.06) 2.0	4.33 (0.05) 56.0	6.58 (0.07) 5.91 (0.09)	
5:2	4.39 (0.06) 3.0	4.47 (0.08) 56.0	6.50 (0.03) 6.06 (0.09)	
6:2	4.51 (0.05) 3.0	4.39 (0.10) 56.0	6.60 (0.04) 6.04 (0.08)	
7:2	4.52 (0.03) 3.0	4.71 (0.07) 56.0	6.59 (0.07) 6.38 (0.07)	

^aFigures in parentheses indicate the standard errors on the fitted parameter values (derived from the least-squares variance–covariance matrix). Data taken from ref 38.

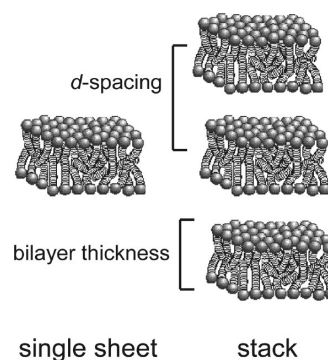


Figure 6. Schematic representation of a single planar lipid bilayer (or sheet) and a stack of bilayers. The *d*-spacing is the sum of the thickness of the lipid bilayer (denoted *L*) and the water layer between the bilayers.

structures, i.e. stacks with a large number of repeats together with an additional factor to take into account Porod scattering. The large Bragg peak observed in the LD complexes at a *Q* value $\sim 0.1 \text{ \AA}^{-1}$ (or 1 nm^{-1}) is indicative of a regularly repeating structure, the *d*-spacing of which can be calculated from the *Q* value at the position of the peak as well as from modeling of the data. We have previously interpreted³⁸ the repeat structure of the LD complexes as large structures of alternating layers of lipid (in the form of a bilayer) and hydrated DNA. As can be seen from Table 2, both the thickness of the bilayer and the *d*-spacing are largely unaltered by the presence of pDNA (and indeed ctDNA).

In the present study, in order to determine whether there was any interaction between the preformed cationic vesicles with peptide 8, the SANS data curves obtained for these mixed vesicle: peptide systems were analyzed using the same parameters as were used to successfully model the vesicles alone (Table 2). It should be noted that the vesicles were the same vesicles as were used to prepare the vesicle:peptide mixture and the LD and LPD complexes. A very good fit to the experimental data was obtained in this way suggesting that either the peptide did not interact with the vesicles or, if it did so, did not significantly alter the structure of the vesicle bilayer. Due to the positively charged nature of both the vesicles and the peptide it is considered that the former option is the most likely.

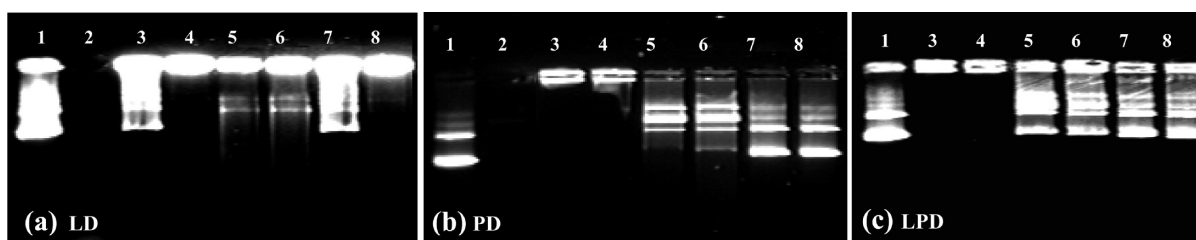


Figure 7. Gel retardation and protection assay of (a) LD complexes using pDNA and Z-9 (4 + 2) at 4:1 (lane 3) and 8:1 (lane 4) weight ratio, (b) PD (8) at 4:1 (lane 3) and 2:1 (lane 4) weight ratios and (c) LPD using (4 + 2):8:pDNA at 2:4:1 (lane 3) and 2:2:1 (lane 4) weight ratios. Protection of the above respective samples from DNase I degradation, followed by pDNA release in the presence of pAsp, is shown in lanes 5 and 6 respectively. Release in the presence of pAsp only is shown in lanes 7 and 8 respectively. (c) Lanes 1 and 2 show controls of free pDNA and pDNA treated with DNase I respectively.

Unlike the LD complexes, the SANS profiles obtained for the LPD complexes show no Bragg peak and could be very well fitted using the parameters used to fit the vesicles from which they were prepared, suggesting that the outer layer of the LPD complexes was composed of a bilayer of similar structure to the vesicles from which they were prepared. However, as the negative staining electron microscopy study showed the presence of electron dense material inside the LPD complexes, assumed to be DNA condensed by the presence of peptide, attempts were made to model the SANS data obtained for the LPD complexes as core-shell particles; however this was unsuccessful.

A probable explanation to that apparent discrepancy between the analysis of the SANS data and the electron microscopy study is that the electron microscopy studies are more sensitive to the presence of DNA than the SANS experiments, and that the DNA was “effectively invisible” when examining the complexes using SANS. This difference in sensitivity arises because the “heavy” phosphorus atom present in DNA will readily scatter electrons (the electron scattering “power” of an element depending upon its atomic weight) and is therefore visible when the LPD complexes are examined using TEM, while the neutron scattering “power” of DNA (expressed as the scattering length density, SLD of the molecule) is, at $4.46 \times 10^{-6} \text{ \AA}^{-2}$ when dispersed in D_2O , not too different from that of D_2O , $6.35 \times 10^{-6} \text{ \AA}^{-2}$, used as the continuous phase in the SANS studies. This means if we assume that hydrated DNA and free D_2O are both present in the central core of the LPD complex (as suggested by our electron microscopy studies), and that this core is surrounded by a bilayer of hydrogenous lipid, with the whole LPD complex dispersed in D_2O , then the difference in the SLD of the LPD core and the D_2O acting as the continuous phase is relatively low, especially when compared to the SLD of the lipid bilayer ($\sim 0.27 \times 10^{-6} \text{ \AA}^{-2}$). As a consequence, therefore, the neutrons do not “see” the DNA in the core of the LPD complexes but only the lipid bilayer which surrounds it, thereby explaining why the SANS data obtained for the LPD complexes were well fitted using the same mixed sheet and stack model as for the parent vesicles.

Note that this explanation of the SANS data does not account for the effect of the presence of peptide 8 on the SLD of the various parts of the LPD complex. In fact the SLD of peptide at about $2.0 \times 10^{-6} \text{ \AA}^{-2}$ is lower than that of D_2O solvated DNA, although the SLD of the protein when solvated with D_2O will increase to at least $3.0 \times 10^{-6} \text{ \AA}^{-2}$, due to hydrogen–deuterium exchange of labile protons. If solvated protein is present in the core of the LPD complex, it would be expected to reduce the SLD of the core slightly further. Our earlier work,³¹ using a combination of fluorescence correlation spectroscopy, fluorescence quenching

experiments and electron microscopy studies, showed that only about 75% of the peptide is associated with an LPD complex formed from a 1:1 molar ratio of DOTMA:DOPE, peptide 8 and pDNA (pCILuc). Furthermore, not all of the peptide was contained within the core of the LPD complex as some of the peptide 8 (thought to be predominately the targeting moiety) passes through the lipid bilayer and is exposed on the exterior surface of the LPD complex.³¹ The combination of these factors explains why the analysis of the present SANS data does not reveal the presence of material (namely, DNA and protein) in the core of the LPD complex while the electron microscopy study does.

The SANS study suggests that there is a lipid bilayer on the outside of the LPD complex, a result in agreement with earlier fluorescence quenching and fluorescence correlation spectroscopy (FCS) measurements on similar integrin targeting LPD complexes.³¹ Interestingly, since LPD complexes were first described in the mid 1990s very little research, other than that reported in ref 31, has been undertaken to establish the detailed molecular architecture of the complexes. The present SANS studies indicate that there are no large changes in the structure of this bilayer when compared to that seen when the lipids were in the form of vesicles. However, as the present SANS studied used only one contrast, namely, hydrogenous lipid and DNA and D_2O , it is not possible to determine whether there were subtle differences in the architecture of the lipid bilayer when in the form of an LPD complex. In order to probe the presence of such changes, a series of contrast variation experiments intended to highlight specific components of the LPD complexes would need to be performed to establish whether or not this was the case.

4.6. Gel Retardation and Protection Assay. Gel electrophoresis experiments were performed to determine the efficiency of pDNA complexation (LD and LPD) and the level of protection complexation affords pDNA from degradation by the enzyme, DNase I. In addition, the extent of pDNA release from DNase I treated and untreated LD and LPD complexes was determined in the presence of polyaspartic acid (pAsp), which should displace and, therefore, release pDNA from the complex. The same experiments were also repeated for complexes prepared using ctDNA. The results obtained for the ctDNA are not reported as they were very similar to those obtained using the LPD complexes prepared using pDNA.

Figures 7a, 7b, and 7c show the results of the gel retardation and protection assays for LD, PD, and LPD complexes prepared using vesicles made from 4 in combination with 2 and pDNA and, where appropriate, peptide 8. The results shown for the LD complexes are those previously reported by us.³⁸ Figure 7a shows the results obtained for LD complexes prepared at weight ratios

of 4:1 and 8:1 (corresponding to charge ratios of 1:1 and 2:1), Figure 7b shows the PD complexes prepared at 2:1 and 4:1 weight ratios (corresponding to charge ratios of 3:1 and 6:1 respectively) and Figure 7c the LPD complexes prepared at 2:2:1 and 2:4:1 weight ratios (corresponding to charge ratios of 1:6:2 and 1:12:2). Lane 1 in each of the three gels shows free, untreated, pDNA in its supercoiled form (the lowest band), open circular and linear forms (the upper bands) while lane 2 shows an absence of any bands due to the complete digestion of the free, uncomplexed pDNA in the presence of DNase I. It is obvious from lanes 3 and 4 in Figure 7a that the pDNA is largely, if not totally, condensed when present in the LD complex at the 8:1 but not the 4:1 weight ratio. This observation is in agreement with earlier zeta potential experiments³⁸ which suggest that insufficient cationic lipid is present to condense all the DNA at the 4:1 weight ratio since a negative zeta potential was measured for the complexes prepared at this composition (see also Table 1).

Upon treating both the LD complexes with pAsp, in the absence of DNase I, as expected in lane 7 a high level of (apparent) pDNA release was observed due to the fact that most of the pDNA was not condensed in the LD complex prepared using the 4:1 weight ratio. In contrast a poor amount of pDNA release was observed with the LD complex prepared using the 8:1 weight ratio in lane 8, possibly explaining the lower transfection efficiency seen with this complex³⁸ as it is essential that the pDNA dissociates from the LD complex within the cell in order for efficient gene transfer to occur. Poor release is one of the reasons why LD complexes may not be very effective transfection agents. For example Pollard et al.⁴⁶ have shown that microinjections of cationic lipid complexed plasmid DNA into the cytoplasm resulted in poor DNA uptake into the nucleus while no transgene expression was observed when the same LD complexes were injected directly into the nucleus. These observations were attributed to poor DNA release from the complex. On the other hand, DNA nuclear localization and transcription were enhanced upon cytoplasmic and nuclear injections of complexes of DNA with either of the polymers polyethyleneimine or polylysine, suggesting that, for good transfection, complete DNA dissociation is required from lipidic vectors, but not from polymeric or peptide vectors, possibly explaining why the LPD complexes are so efficient at transfection.

In addition to poor pDNA release from the 4:1 weight ratio LD complex, extensive pDNA degradation was observed when both the 4:1 and 8:1 weight ratio LD complexes were incubated with DNase I (lanes 5 and 6). Indeed no pDNA in its supercoiled form was detected (as indicated by the arrows), although some DNA was detected in its relaxed circular and linear forms. This is thought to be directly related to the DNase I mechanism of action which initially cuts one of the DNA double strands converting any supercoiled to relaxed circular and the linear forms before eventually degrading the whole DNA.⁴⁷ The degradation of the supercoiled form of pDNA is a very significant observation since the supercoiled form has been reported to be the most bio-active^{47–49} and therefore degradation of this form of DNA in the extracellular space or the cell cytoplasm would significantly hinder transfection efficiency.^{4,50,51}

Figure 7b shows the corresponding PD results obtained when peptide 8 alone was used to condense the pDNA at peptide to pDNA weight ratios of 4:1 and 2:1. Lanes 3 and 4 illustrate that almost complete condensation of pDNA occurred at both weight ratios. Although good DNA release was achieved in the presence of pAsp (lanes 7 and 8), some supercoiled pDNA degradation

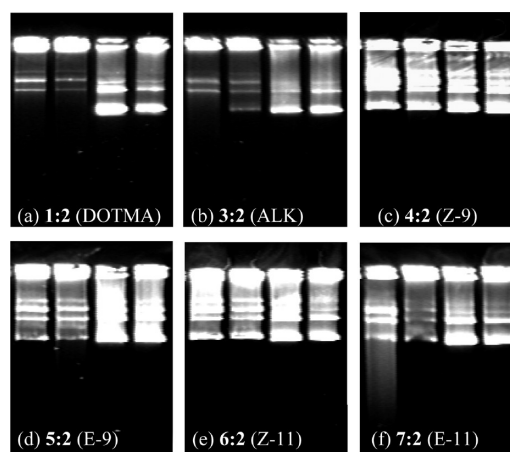


Figure 8. Gel protection and release assay. Protection of pDNA from DNase I degradation by LPD complexes, followed by the release of pDNA with pAsp (lanes 1 and 2) or pAsp only for release comparison (lanes 3 and 4). LPD complexes were prepared using peptide 8 and the following lipids: (a) 1:2 (DOTMA), (b) 3:2 (ALK), (c) 4:2 (Z-9), (d) 5:2 (E-9), (e) 6:2 (Z-11) and (f) 7:2 (E-11) at weight ratios of 2:4:1 (lanes 1 and 3) and 2:2:1 (lanes 2 and 4).

was evident in the presence of DNase I (lanes 5 and 6) as indicated by the faint lowest molecular weight pDNA (indicated by the arrows). Regardless, the level of protection afforded by 8 was greater than that afforded by the LD complexes.

The results obtained for the LPD complexes prepared using 4 are shown in Figure 7c. Complete condensation of pDNA was observed using LPD complexes at both 2:4:1 and 2:2:1 weight ratios (lanes 3 and 4 respectively). Furthermore, as can be seen in lanes 7 and 8, both LPD complexes allowed the complete release of the pDNA while almost completely protecting the pDNA against enzymatic degradation by DNase I as seen in lanes 6 and 7. This conclusion was supported by the preservation of the bands, particularly the lowest band which indicates high level of protection of the supercoiled form of the plasmid, which showed a similar intensity to the controls, i.e. the release in the presence of only pAsp (lanes 7 and 8) and the free, uncomplexed pDNA (lane 1). These results suggest that the LPD complexes exhibit superior condensation and protection of the pDNA when compared to either lipid or peptide component used alone, as well as demonstrating superior pDNA release from the complex in the presence of pAsp. These properties are undoubtedly important contributing factors to the very much superior transfection efficiency observed for the LPD vectors.

The above experiments were repeated for LD, PD and LPD complexes containing the other lipids. The results obtained for the LPD complexes prepared using all the rest of the lipids are shown in Figure 8 while the results obtained for the other LD complexes have been previously reported.³⁸ By and large the results obtained with the other lipids showed similar trends. For example, all LD complexes exhibited extensive pDNA degradation, low release and poor protection of pDNA, similar to that seen above, although there were slight differences in the results as a function of LD weight ratio, which explained the differences in the levels of transfection seen for LD complexes.³⁸ In particular, the LD complexes prepared using the *E*-lipids, which were the most effective at complexing DNA, exhibited the greatest levels of transfection in the MDA-MB 231 cells.

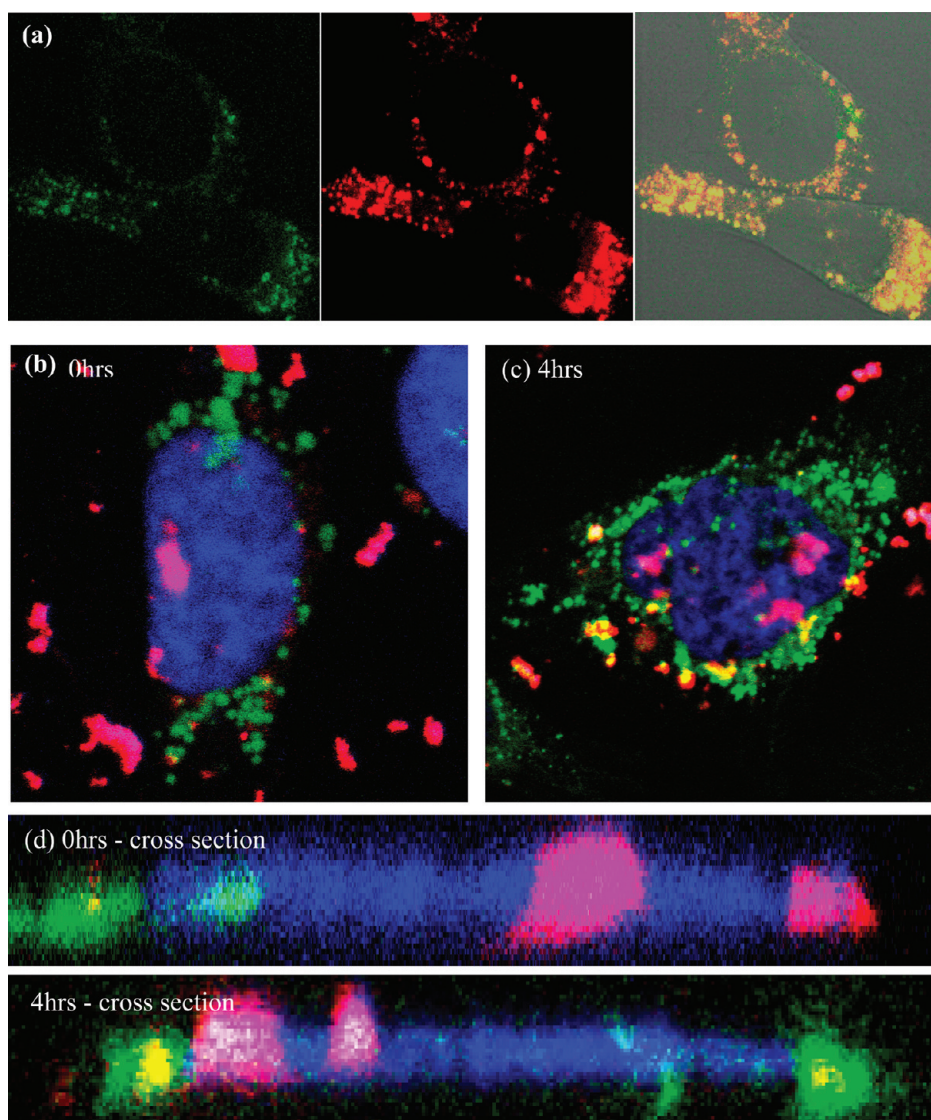


Figure 9. Confocal fluorescence microscopy studies in MDA-MB-231 cells transfected with (a) LD complexes prepared using 7 and 2 and containing 10% BODIPY labeled HPC (green) and rhodamine-labeled pDNA (red) at a 4:1 weight ratio, 10 h after an initial 4 h incubation with the LD complexes; (b) LPD complexes prepared using 4 and 2 and containing 10% BODIPY-labeled HPC (green), unlabeled peptide 8 and rhodamine-labeled pDNA (red) at 2:4:1 weight ratio. The cell nucleus was stained with DAPI (blue). Cells were fixed at (b) 0 h and (c) 4 h after an initial 4 h incubation with the LPD complexes; (d) a cross-sectional XZ plane image of the same cells taken at 0 and 4 h after initial incubation, respectively, to show the nuclear localization of DNA.

In contrast, the LPD complexes prepared in the present study exhibit a clear relationship between the structure of the lipid used to prepare the complex, the level of pDNA protection the corresponding LPD complex afforded and the transfection efficiency obtained for the complex. Figure 8 shows the results obtained for the gel protection and retardation assay using LPD complexes prepared from the cationic lipids 1 and 3–7 (in combination with 2) at weight ratios of 2:2:1 and 2:4:1. Lanes 1 and 2 in each figure show the level of pDNA protection afforded by the LPD complexes formed at the two different mixing ratios in the presence of DNase I, followed by the release of pDNA in the presence of pAsp, while lanes 3 and 4 show the release obtained from the complex in the presence of pAsp. (It should be noted that, regardless of lipid and composition, all the LPD formulations tested showed complete DNA condensation similar to that shown by lipid 4 in lanes 2 and 3 of Figure 7c.) As can be seen

from lanes 1 and 2, LPD complexes prepared using the Z-lipids allowed the complete release of the pDNA while almost completely protecting the pDNA against enzymatic degradation by DNase I. This conclusion was supported by the preservation of the bands, particularly the lowest supercoiled pDNA band which showed a similar intensity to the controls, i.e. the release in the presence of only pAsp (lanes 3 and 4). The level of protection afforded by the other lipids, i.e. the *E*-lipids and the alkyne lipid, was lower. This observation is significant since LPD formulations prepared using the Z-lipids (4 and 6) consistently showed superior transfection to those prepared using the other lipids.

4.7. Confocal Fluorescence Internalization Studies. In order to determine the localization and intracellular fate and trafficking of the various components of the LD and LPD complexes inside the MDA-MB 231 cells, confocal fluorescence microscopy studies were performed. The complexes were prepared containing

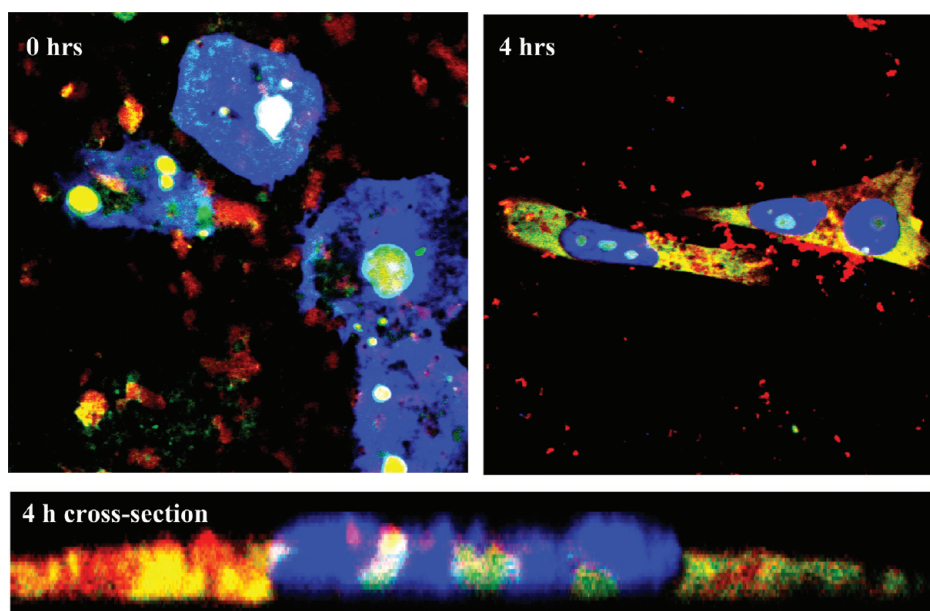


Figure 10. Confocal fluorescence microscopy of MDA-MB-231 cells transfected with LPD complexes prepared using unlabeled Z-9 (4 + 2), labeled peptide 9 (green) and rhodamine-labeled pDNA (red) at 2:4:1 weight ratio. The cell nucleus was stained with DAPI (blue). Cells were fixed at 0 and 4 h after an initial 4 h incubation period. A cross-sectional XZ plane image of the same cells was taken at 4 h to show the nuclear localization of DNA and peptide 8 in relation to the nucleus.

fluorescently labeled components, namely, BODIPY-labeled lipid, a fluorescent analogue of peptide 9 and a rhodamine-labeled pDNA.

The fate in MDA-MB 231 cells of LD complexes prepared using cationic lipid 7 and 2 and incorporating (red) rhodamine-labeled pDNA and (green) BODIPY-labeled lipid with time was determined. The results obtained for the other LD complexes were reported previously.³⁸ Confocal images were taken up to 10 h after an initial incubation period, which consisted of 4 h contact between the LD or LPD complexes and cells. The results obtained for the LD complexes prepared using lipids 7:2 (i.e., the LD complex which showed the greatest levels of transfection) 10 h after the initial incubation are shown in Figure 9a. As can be seen, the lipid and the pDNA predominantly colocalized in spherical endosomal compartments within the perinuclear region of the cell. Similar images were also obtained³⁸ at the earlier time points of 0 and 4 h after the original 4 h incubation period with the complex. Very little fluorescence (of any color) was detected in the nuclear region, suggesting poor pDNA delivery to the nucleus. This low uptake by the nucleus was most probably due to poor endosomal release and/or pDNA degradation in the endosomal/lysosomal compartment and/or the inability of pDNA to traverse the nuclear membrane. This poor nuclear localization translated into a relatively low level of transfection for the LD complexes. Confocal images taken at 24 and 48 h postincubation showed a more diffuse and faded pattern of fluorescence with no improvement in nuclear import (data not shown). Despite minor differences in the colocalization of the fluorescence, broadly similar results were obtained for the lipids 1 and 3–6, with no nuclear import being observed with any of the LD formulations.³⁸

Figure 9b shows the confocal results obtained for the LPD complexes exhibiting the highest level of transfection, namely, those prepared using 4 (Z-9) with 2 and incorporating (green) BODIPY-labeled lipid, (red) rhodamine-labeled pDNA and unlabeled peptide 8. In these experiments the nucleus has been highlighted blue by DAPI staining. As can be seen, a very different

pattern of distribution was observed in that cells examined immediately after the 4 h incubation with the LPD complexes exhibited very little colocalization of the pDNA and the lipid in the cytoplasm, rather the lipid was seen to be predominantly located in endocytic vesicles, whereas in contrast the pDNA was released from the complex and endocytic vesicles and had been internalized into the nuclear region. A similar image was seen when the cells were visualized 4 h later, after the completion of the 4 h incubation period (Figure 9c). XZ cross-sectional images of the same cells at both the 0 and 4 h time points (Figure 9d) confirmed the incorporation of pDNA within the nucleus, excluding the possibility of the pDNA being located above or below the nuclear region. Similar images, all showing detectable amounts of pDNA internalization in the nucleus, were observed for the LPD complexes prepared using the other lipids 1 and 5–7 (shown in Figure 3 in the Supporting Information).

Another set of experiments were performed, designed to determine the localization and intracellular trafficking of the targeting peptide in relation to the pDNA. In this instance (green) Rhodamine green-labeled peptide, 9, and (red) rhodamine-labeled pDNA were used to prepare the complex together with unlabeled lipids 4 and 2. In these experiments the nucleus has also been highlighted blue by DAPI staining. Figure 10 shows again that the pDNA has been incorporated into the nucleus, however, a different pattern of peptide distribution was observed compared to that of the lipid (shown in Figure 9b,c). Interestingly, (some of) the peptide was seen to have trafficked to the nucleus with the pDNA (shown in white due to the colocalization of all three colors). In addition, peptide was seen to be dispersed within the cell cytoplasm rather than being confined to endosomal compartments, as was the case for the lipid. An XZ cross section taken 4 h after incubation also supported the hypothesis of a high level of colocalization of the pDNA with the peptide both in the nucleus and in the cytoplasm. It is therefore possible that the targeting peptide facilitates pDNA

entry into the cell nucleus possibly by acting as a nuclear localization agent.

It is not yet known whether the dissociation of the pDNA from the peptide is required for efficient DNA expression, however, it is obvious that the presence of peptide in the LPD complex has facilitated both the early endosomal release and nuclear localization of pDNA, both of which are known to be crucial for successful transfection efficiency.

This data obtained in both the confocal studies and gel electrophoresis studies tend to support the observation made by Pollard et al.,⁴⁶ who suggested that poor DNA release from cationic lipid complexes is responsible for the poor nuclear localization obtained with these complexes. Furthermore they suggested that nuclear localization of polymer or peptide:DNA complexes (but not lipid:DNA complexes) can result in the high level of DNA transcription. From our earlier³⁸ and present studies it can be seen that the LD complexes poorly release pDNA and furthermore most of the lipid inside the cells is present inside endocytic vesicles.

In contrast, the presence of peptide in a complex is seen to enhance the entry of the pDNA into the cell nucleus. Therefore the combination of lipid and peptide in an LPD complex, together with the modulation of targeting of integrin receptors, may be responsible for the much enhanced transfection observed when lipid and peptide are combined in an LPD complex as opposed to either an LD or PD complex.

5. DISCUSSION

In our earlier study³⁸ we have reported the physicochemical properties, molecular architecture and transfection efficiency of LD complexes formed from a series of structurally related C14 glycerol-based lipids (incorporating *cis*, *trans* and alkyne moieties) when formulated at a 1:1 weight ratio with DOPE. Interestingly, despite very small structural differences between the lipids, very pronounced effects were observed on the level of transfection achieved in breast cancer MDA-MB 231 cells. In particular, the LD complexes prepared from the *E*-lipids were more effective transfection agents than those containing either of the *Z*-lipids or the alkyne lipid. Zhu et al.⁵² recently made a similar observation when studying the behavior of LD complexes prepared from pyridinium based lipids where the *trans* isomer showed a higher transfection efficiency than its *cis* counterpart. The reason for these differences is thought to be primarily a consequence of the ability of the *E*-lipids to better complex DNA, most probably due to the area per molecule of *E*-lipid containing bilayers having the charge distribution matching closest to that of DNA: due to their *trans* conformation, the bilayer containing the *E*-lipids would be expected to be the most closely packed.^{53–55}

In the present study, we have performed similarly detailed experiments on the LPD complexes formed by the same series of lipids, but containing a bifunctional targeting peptide designed to both condense the DNA through its K₁₆ (lysine-rich) region, and to facilitate integrin-specific receptor mediated endocytosis via a peptide sequence that targets $\alpha_3\beta_1$ integrin receptors.^{25–28,31,32,39,41} Significantly, the resulting LPD complexes were shown to possess a far superior transfection efficiency when compared to their LD or PD counterparts. As was seen in our earlier studies investigating the LD complexes, the nature of the lipid used to prepare the complex influenced transfection efficiently, but in this case it was the LPD complexes prepared using *Z*-lipids that were the most effective transfection agents.

It was clear from the confocal fluorescence studies examining the fate of the complexes within the cell after 4 h incubation that,

once in the cell, the LPD complexes underwent dissociation, with the lipid being confined to the endocytic vesicles, while the DNA had clearly internalized into the cell nucleus. Additionally, labeled peptide 9 was shown to be released from the endosomal compartments, since it has distributed throughout the cytoplasm, but also was clearly detected in the nucleus with the DNA, suggesting it might have nuclear import-enhancing properties. In contrast, once in the cell, the components of the LD complexes were highly colocalized and confined to endosomal compartments with very little evidence of nuclear DNA import.

The combination of the dynamic light scattering and zeta potential measurements, together with the TEM and SANS studies, lead to the hypothesis that the LPD complexes prepared in the present study all contained a central core of DNA surrounded by a lipid bilayer. This proposed structure is in close agreement with that proposed by Mustapa et al.³¹ based on fluorescence quenching studies of LPD complexes prepared using DOTMA:DOPE 1:1 and containing peptide 8. In their study, these workers concluded that the lysine-rich portion of the peptide interacts with DNA, resulting in a tightly bound inner core of peptide:DNA complex, which is then surrounded by the lipid bilayer, from which the integrin-targeting sequence of the peptide partially protrudes, allowing it to interact with its target receptors.

In the LPD system, the protrusion of the targeting sequence CRRETAWAC of peptide 8 on the surface of the complex³¹ is believed to be crucial for the targeting and synergistic activity of the LPD complex. Indeed, when the amount of lipid in an LPD formulation composed of DOTMA:DOPE is increased from 2:4:1 to 4:4:1 and 6:4:1 weight ratios, the transfection efficiency decreases from 100% to 65% and 40%, respectively (unpublished data). This reduction in transfection is most likely a consequence of the shielding of the targeting portion of the peptide by the lipid, probably due to the formation of multiple bilayers surrounding the central core. This observation suggests that it is important to have enough lipid to form a single bilayer on the exterior of the LPD complex but not so much that multiple bilayers are formed. Similarly, the “fluidity” of the lipid bilayer surrounding the core peptide:DNA complex may reasonably be expected to influence the way in which the targeting sequence protrudes from the bilayer. Indeed it is well established that lipids possessing *trans* double bonds in their hydrocarbon chains are straighter in conformation and are therefore packed more closely than the “kinked” *cis* chains, which pack less tightly, resulting in a significantly larger area per molecule (see for example refs 53–55). As a consequence bilayers containing *Z*-lipids are more “fluid” and more permeable than those prepared from *E*-lipids. In the case of the LPD complexes, it may be therefore that the bilayers formed by the *cis* lipids are less tightly packed therefore allowing more of the targeting sequence to protrude, leading to a better targeting and transfection ability. In previous studies,³¹ fluorescence quenching studies on LPD complexes demonstrated that the Trp residue in the center of the CRRETAWAC sequence is more accessible to the solvent, whereas when a fluorophore was attached at the C-terminus, this was partly shielded from the quenching reagent. Subtle variations in the degree to which the CRRETAWAC sequence can protrude from the bilayer, governed by the fluidity of the bilayer, may therefore be crucial to the extent to which the LPD complex can attach to the integrin receptor and be endocytosed.

Another possible explanation for the improved transfection activity of the LPD complexes containing the *cis* as opposed to

trans lipids could be their ability to better protect the DNA from enzymatic degradation as shown by gel electrophoresis. Interestingly, gel electrophoresis experiments investigating the complexation, enzymatic protection and release of DNA from the complexes are the only studies to have directly shown differences with lipid structure for both LD and LPD complexes. Unlike LPD complexes, all LD complexes showed extensive DNA degradation as well as poor DNA release; both properties are considered to be detrimental for efficient gene delivery. Significantly, and in line with the observed transfection efficiencies, the LD complexes containing the trans lipids more efficiently complexed DNA, while in the case of the LPD complexes, those containing the cis lipids were more superior at protecting DNA from enzymatic degradation. This could again be attributed to the higher fluidity of the cis bilayers, in that they would be more accommodating to the protruding targeting peptide than the trans lipids which wish to form more highly ordered structures, therefore possibly resulting in gaps in the bilayer where the peptide sticks out, and as a consequence less of a protective layer around the DNA core.

Overall, we conclude that the incorporation of a bifunctional DNA-binding and receptor targeting peptide in the LD formulation has had a dramatic effect on the transfection activity, the complex structure and its distribution inside the cell. The geometry of the lipids used influenced transfection significantly in both LD and LPD complexes, although the differences in structural properties between lipoplex and lipopolyplex formulations dictated which type of lipid had greater success in delivering the DNA. In the case of LD complexes, the more tightly packed trans lipids conferred superior activity due to better DNA condensation as a result of more optimal packing in relation to the DNA molecule, whereas, in the case of the LPD complexes, the more fluid cis lipids conferred better activity, probably due to allowing more of the targeting peptide sequence to protrude, while maintaining superior protection of the DNA from enzymatic degradation.

■ ASSOCIATED CONTENT

S Supporting Information. HPLC and mass spectrometry data for peptides 8, 9, 10 and 11, apparent hydrodynamic sizes of LD and LPD complexes formulated at 0.1 mg/mL, TEM images of LD and LPD complexes prepared with lipids 1 or 3 and pDNA, and confocal fluorescence images of LPD complexes prepared using lipids 1, 5, 6 and 7. This material is available free of charge via the Internet at <http://pubs.acs.org>.

■ AUTHOR INFORMATION

Corresponding Author

*E-mail: Laila.kudsiova@kcl.ac.uk. Institute of Pharmaceutical Science, King's College London, Franklin-Wilkins Building, 150 Stamford Street, Waterloo Campus, London SE1 9NH, U.K. Tel: 02078484812. Fax: 02078484800.

■ ACKNOWLEDGMENT

The Maplethorpe Fellowship, London University, King's College London, and the EPSRC are thanked for support of L. K., J.H., F.C. and K.W. STFC is thanked for the award of neutron beam time at the ISIS Facility, The Rutherford Appleton Laboratories. Simon Richardson is thanked for helpful discussions on the cell culture studies. Konstantinos Thalassinou and Richard Kerr (Institute of Structural and Molecular Biology at UCL/

Birkbeck) are thanked for helpful discussions and the mass spectrometry data for peptide 9.

■ REFERENCES

- (1) Somia, N.; Verma, I. M. Gene therapy: trials and tribulations. *Nat. Rev. Genet.* **2000**, *1*, 91–99.
- (2) Davis, M. E. Non-viral gene delivery systems. *Curr. Opin. Biotechnol.* **2002**, *13*, 128–131.
- (3) Niidome, T.; Huang, L. Gene therapy progress and prospects: Nonviral vectors. *Gene Ther.* **2002**, *9*, 1647–1652.
- (4) Wiethoff, C. M.; Middaugh, C. R. Barriers to nonviral gene delivery. *J. Pharm. Sci.* **2003**, *92*, 203–217.
- (5) Middaugh, C. R.; Ramsey, J. D. Analysis of cationic-lipid-plasmid-DNA complexes. *Anal. Chem.* **2007**, *79*, 7240–7248.
- (6) Braun, C. S.; Jas, G. S.; Choosakoonkriang, S.; Koe, G. S.; Smith, J. G.; Middaugh, C. R. The structure of DNA within cationic lipid/DNA complexes. *Biophys. J.* **2003**, *84*, 1114–1123.
- (7) Miller, A. D. Cationic liposomes for gene therapy. *Angew. Chem., Int. Ed.* **1998**, *37*, 1768–1785.
- (8) Varga, C. M.; Wickham, T. J.; Lauffenburger, D. A. Receptor-mediated targeting of gene delivery vectors: Insights from molecular mechanisms for improved vehicle design. *Biotechnol. Bioeng.* **2000**, *70*, 593–605.
- (9) Miller, A. D. The problem with cationic liposome/micelle-based non-viral vector systems for gene therapy. *Curr. Med. Chem.* **2003**, *10*, 1195–1211.
- (10) Düzgünes, N.; Tros de Ilarduya, C.; Simões, S.; Zhdanov, R.; Konopka, K.; Pedrosa de Lima, M. Cationic Liposomes for Gene Delivery: Novel Cationic Lipids and Enhancement by Proteins and Peptides. *Curr. Med. Chem.* **2003**, *10*, 1213–1220.
- (11) Maruyama, K. PEG-Immunoliposomes. *Biosci. Rep.* **2002**, *22*, 251–266.
- (12) Demeneix, B.; Hassani, Z.; Behr, J. P. Towards multifunctional synthetic vectors. *Curr. Gene Ther.* **2004**, *4*, 445–455.
- (13) Schatzlein, A. G. Targeting of synthetic gene delivery systems. *J. Biomed. Biotechnol.* **2003**, *2*, 149–158.
- (14) Wadhwa, M. S.; Collard, W. T.; Adami, R. C.; McKenzie, D. L.; Rice, K. G. Peptide-mediated gene delivery: influence of peptide structure on gene expression. *Bioconjugate Chem.* **1997**, *8*, 81–88.
- (15) McKenzie, D. L.; Kwok, K. Y.; Rice, K. G. A potent new class of reductively activated peptide gene delivery agents. *J. Biol. Chem.* **2000**, *275*, 9970–9977.
- (16) McKenzie, D. L.; Collard, W. T.; Rice, K. G. Comparative gene transfer efficiency of low molecular weight polylysine DNA-condensing peptides. *J. Pept. Res.* **1999**, *54*, 311–318.
- (17) Adami, R. C.; Collard, W. T.; Gupta, S. A.; Kwok, K. Y.; Bonadio, J.; Rice, K. G. Stability of peptide-condensed plasmid DNA formulations. *J. Pharm. Sci.* **1998**, *87*, 678–683.
- (18) Hart, S. L. Integrin-mediated vectors for gene transfer and therapy. *Curr. Opin. Mol. Ther.* **1999**, *1*, 197–203.
- (19) Hart, S. L.; Collins, L.; Gustafsson, K.; Fabre, J. W. Integrin-mediated transfection with peptides containing arginine-glycine-aspartic acid domains. *Gene Ther.* **1997**, *4*, 1225–1230.
- (20) Martin, M. E.; Rice, K. G. Peptide-guided gene delivery. *AAPS J.* **2007**, *9*, E18–E29.
- (21) Liu, X.; Tian, P. K.; Ju, D. W.; Zhang, M. H.; Yao, M.; Cao, X. T.; Gu, J. R. Systemic genetic transfer of p21WAF-1 and GM-CSF utilizing of a novel oligopeptide-based EGF receptor targeting polyplex. *Cancer Gene Ther.* **2003**, *10*, 529–539.
- (22) Wolschek, M. F.; Thallinger, C.; Kurs, M.; Rossler, V.; Allen, M.; Lichtenberger, C.; Kircheis, R.; Lucas, T.; Wilhelm, M.; Reinisch, W.; Gangl, A.; Wagner, E.; Jansen, B. Specific systemic nonviral gene delivery to human hepatocellular carcinoma xenografts in SCID mice. *Hepatology* **2002**, *36*, 1106–1114.
- (23) Kostarelos, K.; Miller, A. D. Synthetic self-assembly ABCD nanoparticles; a structural paradigm for viable synthetic non-viral vectors. *Chem. Soc. Rev.* **2005**, *34*, 970–994.

- (24) Tagawa, T.; Manvell, M.; Brown, N.; Keller, M.; Perouzel, E.; Murray, K. D.; Harbottle, R. P.; Tecle, M.; Booy, F.; Brahimi-Horn, M. C.; Coutelle, C.; Lemoine, N. R.; Alton, E. W. F.; Miller, A. D. Characterisation of LMD virus-like nanoparticles self-assembled from cationic liposomes, adenovirus core peptide μ (mu) and plasmid DNA. *Gene Ther.* **2002**, *9*, 564–576.
- (25) Hart, S. L.; Arancibia-Carcamo, C. V.; Wolfert, M. A.; Mailhos, C.; O'Reilly, N. J.; Ali, R. R.; Coutelle, C.; George, A. J. T.; Harbottle, R. P.; Knight, A. M.; Larkin, D. F. P.; Levinsky, R. J.; Seymour, L. W.; Thrasher, A. J.; Kinnon, C. Lipid-Mediated Enhancement of Transfection by a non-viral Integrin-Targeting Vector. *Hum. Gene Ther.* **1998**, *9*, 575–585.
- (26) Jenkins, R. G.; Herrick, S. E.; Meng, Q. H.; Kinnon, C.; Laurent, G. J.; McAnulty, R. J.; Hart, S. L. An integrin-targeted non-viral vector for pulmonary gene therapy. *Gene Ther.* **2000**, *7*, 393–400.
- (27) Parkes, R.; Meng, Q. H.; Siapati, K. E.; McEwan, J. R.; Hart, S. L. High efficiency transfection of porcine vascular cells in vitro with a synthetic vector system. *J. Gene Med.* **2002**, *4*, 292–299.
- (28) Writer, M.; Hurley, C. A.; Sarkar, S.; Copeman, D. M.; Wong, J. B.; Odlyha, M.; Lawrence, M. J.; Tabor, A. B.; McAnulty, R. J.; Shamlou, P. A.; Hailes, H. C.; Hart, S. L. Analysis and optimization of the cationic lipid component of a lipid/peptide vector formulation for enhanced transfection in vitro and in vivo. *J. Liposome Res.* **2006**, *16*, 373–389.
- (29) Irvine, S. A.; Meng, Q. H.; Afzal, F.; Ho, J.; Wong, J. B.; Hailes, H. C.; Tabor, A. B.; McEwan, J. R.; Hart, S. L. Receptor targeted nanocomplexes optimized for gene transfer to primary vascular cells and explant cultures of rabbit aorta. *Mol. Ther.* **2008**, *16*, 508–515.
- (30) Writer, M. J.; Marshall, B.; Pilkington-Miksa, M. A.; Barker, S. E.; Jacobsen, M.; Bell, P. C.; Lester, D. H.; Tabor, A. B.; Hailes, H. C.; Klein, N.; Hart, S. L. Targeted gene delivery to human airway epithelial cells with synthetic vectors incorporating novel targeting peptides selected by phage display. *J. Drug Targeting* **2004**, *12*, 185–193.
- (31) Mustapa, M. F. M.; Bell, P. C.; Hurley, C. A.; Nicol, A.; Guenin, E.; Sarkar, S.; Writer, M. J.; Barker, S. E.; Wong, J. B.; Pilkington-Miksa, M. A.; Papahadjopoulos-Sternberg, B.; Shamlou, P. A.; Hailes, H. C.; Hart, S. L.; Zicha, D.; Tabor, A. B. Biophysical characterization of an integrin-targeted lipopolyplex gene delivery vector. *Biochemistry* **2007**, *46*, 12930–12944.
- (32) Pilkington-Miksa, M. A.; Writer, M. J.; Sarkar, S.; Meng, O. H.; Barker, S. E.; Shamlou, P. A.; Hailes, H. C.; Hart, S. L.; Tabor, A. B. Targeting lipopolyplexes using bifunctional peptides incorporating hydrophobic spacer amino acids: synthesis, transfection, and biophysical studies. *Bioconjugate Chem.* **2007**, *18*, 1800–1810.
- (33) Mustapa, M. F. M.; Grosse, S. M.; Kudsiova, L.; Elbs, M.; Raiber, E. A.; Wong, J. B.; Brain, A. P. R.; Armer, H. E. J.; Warley, A.; Keppler, M.; Ng, T.; Lawrence, M. J.; Hart, S. L.; Hailes, H. C.; Tabor, A. B. Stabilized integrin-targeting ternary LPD (lipopolyplex) vectors for gene delivery designed to disassemble within the target cell. *Bioconjugate Chem.* **2009**, *20*, 518–532.
- (34) Pilkington-Miksa, M. A.; Sarkar, S.; Writer, M. J.; Barker, S. W.; Ayazi Shamlou, P.; Hart, S. L.; Hailes, H. C.; Tabor, A. B. Synthesis of bifunctional integrin-binding peptides containing PEG spacers of defined length for non-viral gene delivery. *Eur. J. Org. Chem.* **2008**, *17*, 2900–2914.
- (35) Tagalakakis, A. D.; McAnulty, R. J.; Devaney, J.; Bottoms, S. E.; Wong, J. B.; Elbs, M.; Writer, M. J.; Hailes, H. C.; Tabor, A. B.; O'Callaghan, C.; Jaffe, A.; Hart, S. L. A receptor-targeted nanocomplex vector system optimized for respiratory gene transfer. *Mol. Ther.* **2008**, *16*, 907–915.
- (36) Hurley, C. A.; Wong, J. B.; Ho, J.; Writer, M.; Irvine, S. A.; Lawrence, M. J.; Hart, S. L.; Tabor, A. B.; Hailes, H. C. Mono- and dicationic short PEG and methylene dioxyalkylglycerols for use in synthetic gene delivery systems. *Org. Biomol. Chem.* **2008**, *6*, 2554–2559.
- (37) Wong, J. B.; Grosse, S.; Tabor, A. B.; Hart, S. L.; Hailes, H. C. Acid cleavable PEG lipids for applications in a ternary gene delivery vector. *Mol. Biosyst.* **2008**, *4*, 532–541.
- (38) Kudsiova, L.; Ho, J.; Fridrich, B.; Harvey, R.; Keppler, M.; Ng, T.; Hart, S. L.; Tabor, A. B.; Hailes, H. C.; Lawrence, M. J. Lipid chain geometry of C14 glycerol-based lipids: Effect on lipoplex structure and transfection. *Mol. Biosyst.* **2011**, *7*, 422–436.
- (39) Hurley, C. A.; Wong, J. B.; Hailes, H. C.; Tabor, A. B. Asymmetric synthesis of sialkyl-3-alkylammonium cationic lipids. *J. Org. Chem.* **2004**, *69*, 980–984.
- (40) Grosse, S. M.; Tagalakakis, A. D.; Mohd Mustapa, M. F.; Elbs, M.; Meng, Q.-H.; Mohammadi, A.; Tabor, A. B.; Hailes, H. C.; Hart, S. L. Tumor-specific gene transfer with receptor-mediated nanocomplexes modified by polyethylene glycol shielding and endosomally cleavable lipid and peptide linkers. *FASEB J.* **2010**, *24*, 2301–2313.
- (41) Koivunen, E.; Wang, B.; Ruoslahti, E. Isolation of a highly specific ligand for the $\alpha 5 \beta 1$ integrin from a phage display library. *J. Cell Biol.* **1994**, *124*, 373–380.
- (42) Kamber, B.; Hartmann, A.; Eisler, K.; Riniker, B.; Rink, H.; Sieber, P.; Rittel, W. The synthesis of cystine peptides by iodine oxidation of S-trityl cysteine and S-acetamidomethylcysteine peptides. *Helv. Chim. Acta* **1980**, *63*, 899–915.
- (43) Harvey, R. D.; Heenan, K.; Barlow, D. J.; Lawrence, M. J. The effect of electrolyte on the morphology of vesicles composed of the dialkyl polyoxyethylene ether surfactant 2C(18)E(12). *Chem. Phys. Lipids* **2005**, *133*, 27–36.
- (44) Heenan, R. K. Data fitting program for small-angle neutron scattering. Rutherford Appleton Laboratory. *RAL Report*. **1989**, 89–129. Available online at <http://www.small-angle.ac.uk/small-angle/Software.html>.
- (45) Matsui, H.; Pan, S. Distribution of DNA in cationic liposome complexes probed by Raman microscopy. *Langmuir* **2001**, *17*, 571–573.
- (46) Pollard, H.; Remy, J. S.; Loussouarn, G.; Demolombe, S.; Behr, J. P.; Escande, D. Polyethylenimine but not cationic lipids promotes transgene delivery to the nucleus in mammalian cells. *J. Biol. Chem.* **1998**, *273*, 7507–7511.
- (47) del Pozo-Rodríguez, A.; Pujals, S.; Delgado, D.; Solinís, M. A.; Gascón, A. R.; Giral, E.; Pedraz, J. L. A proline-rich peptide improves cell transfection of solid lipid nanoparticle-based non-viral vectors. *J. Controlled Release* **2009**, *133*, 52–59.
- (48) Middaugh, C. R.; Evans, R. K.; Montgomery, D. L.; Casimiro, D. R. Analysis of plasmid DNA from a pharmaceutical perspective. *J. Pharm. Sci.* **1998**, *87*, 130–146.
- (49) Remaut, K.; Sanders, N. N.; Fayazpour, F.; Demeester, J.; De Smedt, S. C. Influence of plasmid DNA topology on the transfection properties of DOTAP/DOPE lipopolyplexes. *J. Controlled Release* **2006**, *115*, 335–343.
- (50) Mumper, R. J.; Wang, J.; Klakamp, S. L.; Nitta, H.; Anwer, K.; Tagliaferri, F.; Rolland, A. P. Protective interactive noncondensing (PINC) polymers for enhanced plasmid distribution and expression in rat skeletal muscle. *J. Controlled Release* **1998**, *52*, 191–203.
- (51) Pollard, H.; Toumaniantz, G.; Amos, J. L.; Avet-Loiseau, H.; Guihard, G.; Behr, J. P.; Escande, D. Ca^{2+} -Sensitive cytosolic nucleases prevent efficient delivery to the nucleus of injected plasmids. *J. Gene Med.* **2001**, *3*, 153–164.
- (52) Zhu, L.; Lu, Y.; Miller, D. D.; Mahato, R. I. Structural and formulation factors influencing pyridinium lipid-based gene transfer. *Bioconjugate Chem.* **2008**, *19*, 2499–2512.
- (53) Cevc, G. How Membrane Chain-Melting Phase-Transition Temperature is Affected by the Lipid Chain Asymmetry and Degree of Unsaturation: An Effective Chain-Length Model. *Biochemistry* **1991**, *30*, 7186–7193.
- (54) Roach, C.; Feller, S. E.; Ward, J. A.; Shaikh, S. R.; Zerouga, M.; Stillwell, W. Comparison of *Cis* and *Trans* fatty acid containing phosphatidylcholines on membrane properties. *Biochemistry* **2004**, *43*, 6344–6351.
- (55) Janosi, L.; Gorfe, A. Importance of the Sphingosine Base Double-Bond Geometry for the Structural and Thermodynamic Properties of Sphingomyelin Bilayers. *Biophys. J.* **2010**, *99*, 2957–2966.
- (56) Rich, D. H.; Green, J.; Toth, M. V.; Marshall, G. R.; Kent, S. B. H. Hydroxyethylamine analogues of the p17/p24 substrate cleavage site are tight-binding inhibitors of HIV protease. *J. Med. Chem.* **1990**, *33*, 1285–1288.